TITLE Convective instabilities in binary fluids

AUTHOR David Holton

INSTITUTION and DATE UNIVERSITY WARWICK 1989

Convective instabilities in binary fluids

David Holton

25 January 1989

Contents

Figure 1.

A single fluid in a cylindrical dish heated from below. Flow patterns at several values of ϵ, taken from V. Steinberg et al.(1985). The values of ϵ are (a) 0.29; (b) 0.18; (c) 0.13; (d) 0.08; (e) 0.02; (f) -0.06. Patterns a and b represent concentric flow. For the rest, except (f) the concentric flow is unstable, but the evolution of the pattern is slow and images do not represent a steady state. This figure demonstrates the phenomena of critical slowing down near the point of bifurcation.

Figure 2.

A stable equilibrium

Figure 3.

An asymptotically stable flow

Figure 4.

The roll configuration in a layer of fluid. The various symmetries are shown.

Figure 5.

The pitchfork and broken pitchfork bifurcations.

Figure 6.

Benjamin's apparatus for demonstrating the buckling of a viscoelastic arch of wire (taken from D.D. Joseph (1983))

Figure 7.

The tricritical bifurcation, the arrows indicate the hysteretic phenomena

Figure 8.

Nusselt number verses the reduced Rayleigh number. The solid curve satisfies $Nu - 1 = \left(\frac{R}{4.88}\right)^{0.8}$. Data taken from Gao and Behringer 1986.

Figure 9.

The stability curves (Rayleigh number versus wave number) for the free slip pervious (FSP), no slip impervious (NSI) and free slip impervious (FSI). The critical horizontal wave numbers are shown.

Figure 10.

X versus time at onset of convection for the eight mode problem. It shows the characteristic precipitious relaxation to the oscillatory state. This state becomes unstable to a fixed point.

Figure 11.

X versus time for the fourteen mode problem, the final oscillatory state is stable.

Figure 12.

X_1 versus Y_1 for the five mode model before and after the period doubling bifurcation.

Figure 13.

Schematic representation of the period doubling cascade to the heteroclinic explosion (Moore et al 1983).

Figure 14.

Bifurcation diagram (A vs. λ) in the (a,b) plane, taken from Knobloch et al (1986). Solid lines denote stable solutions, dashed lines indicate unstable solutions.

Figure 15.

Bifurcation diagram showing supercritical ($\psi > \psi_c$), tricritical ($\psi = \psi_c$) and subcritical($\psi < \psi_c$) behaviour.

Memorandum

This dissertation is submitted to the University of Warwick in support of my application for the degree of Doctor of Philosophy. It contains an account of my own work performed at the School of Physics of the University of Warwick under the supervision of Doctor George Rowlands. No part of this thesis has been submitted to this or any other University. The work described in this thesis is the result of my own independent research except where acknowledged in the text.

Acknowledgements

The author wishes to express his thanks to all who made the compilation of this thesis possible. I would especially like to mention Dr. George Rowlands for his supervision and friendship throughout.

I also like to thank Dr J.K. Bhattacharjee and Dr. P Lucas at Manchester University for useful correspondence and suggestions throughout the study of the Hopf bifurcation.

I also gratefully acknowledge the financial support provided by S.E.R.C.

Abstract

The subject of two-dimensional convection in a binary fluid is treated by analytical methods and through Galerkin models. The analysis will focus on describing the dynamics of convection at onset of convection. Two independent dynamical parameters are present- one more degree of freedom than single fluid convection.

We shall derive normal forms for the tricritical bifurcation - describing the transition between a forward and backward pitchfork bifurcation of a two - dimensional array of rolls in a convecting bulk binary fluid mixture. A multiple time perturbation scheme is constructed to fifth order to describe this motion. The coefficients of the equation are determined as a function of the Lewis number (the ratio of the mass to thermal diffusivity). The degenerate Hopf bifurcation is also investigated using a similar perturbative scheme; with a prediction of the coefficients involved.

A model system, using a 'minimal representation'(Veronis 1968) gives rise to a Galerkin truncated scheme (a set of 14 ordinary differential equations). It is claimed that the dynamical character of both the tricritical and degenerate Hopf bifurcation are included in the zoology of the bifurcation behaviour at onset of convection. These and other dynamical aspects of the equations are investigated.

In an attempt to improve upon free slip pervious boundaries a projection of the equations is made onto a more appropriate subspace. A comparison with experimental evidence is given.

Chapter 1 - The Physics of Double Diffusive Convection

1.1 Abstract

This chapter contains the basic physics required to describe the convective process in a binary fluid. The two fluids will be taken to be completely miscible. The basic equations of motion for convection in binary fluids are presented.

1.2 Mechanism for instability

We suppose that an element of binary fluid is displaced vertically in a layer in which the temperature and concentration of one component both increase with height. The presence of this displacement, we assume, is generated through external forcing and will upset local equilibrium. Unforced, diffusive processes will tend to drive the system towards equilibrium (the motionless state) and the motion of the fluid will relax to quiesence. In a non-equilibrium state in which the layer is continually and regularly stressed, by heating from below (the temperature is kept constant at the top and bottom boundaries) we may observe bulk movement of the fluid. The bulk movement of a fluid when it is thermally stressed is called convection. As a particle of displaced fluid is checked (stops rising, losing its thermal buoyancy), moving into a colder region, its composition will also change through diffusion. The diffusion in this case is due to the system

trying to equilibrate local composition. The critical observation is that when the stressed fluid undergoes a convective cycle the particle may end up with a markedly different composition. Hence, it may over or under shoot its original position and undergo oscillatory behaviour. At onset of convection (from the conductive state) we may observe oscillatory behaviour in double diffusive systems (in contrast to a single fluid) due to the fluid motion being unable settle in a steady state configuration due to the element of fluid losing buoyancy through two unequal processes: thermal diffusion and mass diffusion. The mass diffusion may act to enhance or retard convection.

The subsequent spatial pattern we observe is highly dependent upon many factors. Geometry of the cell in which the fluid is contained, its size (aspect ratio) and shape all play an important role in determining the dynamical flavour of the flow. The geometry of the container, will effect the symmetry, if any, of the problem. A number of flow patterns shadowgraphically visualised for a fluid heated from below in a cylindrical dish, obtained from experiment of Steinberg et al 1985, are shown in fig. 1, to show the dynamical variety.

To render analysis tractable, an infinite box or periodic boundary conditions are often used to model experiment. In a finite box, for instance, any translational invariance due to the imposed periodicity will be lost. In the analysis that appears in this thesis the simplest possible configuration,

that of a regular array of roll solutions shown in fig. 4 will be considered, realisable in rectangular boxes in which the rolls align themselves parallel to the shorter side. Other configurations, such as hexagonal or Bénard type cells will not be treated.

To summarise: the underlying mechanism of oscillation is the discrepancy between the relaxation times for thermal and concentration fluctuations. This in turn gives rise to extra dynamical behaviour at the onset of convection.

1.3 Equations of motion

1.3.1 The Navier-Stokes equations

We shall consider a horizontally infinite layer of binary fluid infinite in the lateral direction and of constant thickness d. It will start with linear gradients of temperature and concentration in equilibrium; see equations (11) and (12). This we shall call this the conductive regime. A particle of homogeneous fluid, binary or otherwise, will obey the following equation of Navier-Stokes:

$$\frac{\partial \vec{V}}{\partial t} + \vec{V}.\nabla\vec{V} = -\frac{1}{\rho_m}\vec{\nabla}P + \vec{g}\frac{\rho}{\rho_m} + \nu\nabla^2\vec{V}, \qquad (1)$$

where $\vec{V}$ is the velocity, ρ, ρ_m ,the density and mean density respectively. The other variables are the hydrostatic pressure P, gravitational constant g, and ν kinematic viscosity. We have used the usual Boussinesq approximation (Chandrasekar 1981) in which all of the physical parameters may

be regarded as constants except the density when it multiplies the bulk force term. This approximation seems to be in keeping with most realistic, controlled experiments. Equation (1) is an expression of the conservation of momentum. The only ambiguity, as pointed out in the text book on fluid mechanics by Landau and Lifschitz [1959] is in the definition of velocity for a binary fluid, i.e. which fluid's velocity are we measuring? However, after a moment's thought this ambiguity may be overcome by simply defining the velocity as the momentum density per unit volume divided by density. The left-hand side of equation(1) may be more concisely written in terms of the usual Eulerian description of an 'advective' or total derivative:

$$\frac{D\vec{V}}{Dt} = \frac{\partial \vec{V}}{\partial t} + \vec{V}.\nabla\vec{V}, \qquad (2)$$

as the velocity is a function of space and time. The velocity is a vector quantity $\vec{V}$ = (u,v,w). We will eventually assume that the basic state we are interested in is a roll solution (schematically represented in fig 4), in which we may regard v=0.

A three-dimensional description may be developed through either developing the third dimension as a spatial perturbation on the basic roll solution (Segal 1969) or through imposing a physically realisable three dimensional pattern, e.g. a hexagonal pattern (Hohenberg P.C. and Swift J.B. 1987).

1.3.2 Incompressibility

We assume the fluid to be incompressible. We also assume the fluids are non-reacting and hence, assume there are no chemical processes going on. Consequently, we obtain the result:

$$\bar{\nabla}.\bar{V} = 0, \tag{3}$$

which makes our vector field solenoidal. At this point we may combine equations (1) and (3). This results in expressing the velocity, in the two dimensional case, in terms of a stream function ψ. The velocities in the horizontal and vertical directions can then be written as $\frac{\partial \psi}{\partial x} = v$ and $\frac{\partial \psi}{\partial z} = -u$.

1.3.3 Conservation of Energy

An equation for the temperature may be derived using conservation of energy. We use in its derivation various thermodynamic relations, details of which are given in appendix 1. The equation for the temperature T takes the particularly simple form:

$$\frac{DT}{Dt} = -\frac{1}{\rho_m C_P}\nabla.q. \tag{4}$$

T is the temperature, C_p is the specific heat at constant pressure, and q is the heat flux.

1.3.4 Conservation of species

For a binary fluid we define c to be the concentration of the lighter fluid. The corresponding equation for c is;

$$\frac{Dc}{Dt} = -\frac{1}{\rho_m}\nabla \cdot j, \tag{5}$$

where j is the mass flux of the lighter component. This expression may be generalised to include internal generation of heat. We will however restrict ourselves to realistic experimental circumstances in which we may neglect these generalisations.

1.3.5 The equation of state

One last expression we require to fully describe the equations for the binary fluid is for the density. We adopt the simplest non-trivial equation of state for the density to take into consideration its functional dependence on the temperature and concentration (i.e. the lowest order nontrivial Taylor expansion):

$$\rho = \rho_m[1 - \alpha(T - T_0) - \beta(c - c_0)] \tag{6}$$

where $\alpha = -\frac{1}{\rho}\left(\frac{\partial \rho}{\partial T}\right)_c$ and $\beta = -\frac{1}{\rho}\left(\frac{\partial \rho}{\partial c}\right)_T$, and T_0, c_0 are the temperature and concentration at the bottom boundary and respectively. The notation is classical (Chandrasekar 1981).

What remains is an expression for the phenomenological terms of j and q. Also, an appropriate set of boundary conditions must be specified. The

boundary conditions in the lateral direction are taken as periodic. Periodicity is specified purely for simplicity. Periodic boundary conditions may be thought to be valid for an infinite or sufficiently large box. This intuitive interpretation of the infinite box can be misleading. The horizontal plates that bound the fluid should be take to be rigid and allow no mass flux across the boundary. Rigidity ensures that the normal component of the velocity field at the top and bottom boundaries is zero. These conditions will be relaxed to make the analysis tractable. These approximations will be addressed after the fluxes i and q are given.

1.3.6 Phenomenological effects - the Soret and Dufour effects

The mass diffusion flux i, and the heat diffusion flux q, are due to the presence of temperature and concentration variations in the fluid. One may naively guess that the heat flux is linearly related to the gradient of the temperature; this may be more familiar as a statement of Fourier's law in the conduction of heat down, say a bar of metal. Analogously, the mass flux may be considered proportional to the gradient of the mass distribution (the gradient of concentration). However, this picture is largely incomplete and inaccurate. Generally, each flux will depend on a linear combination of gradients of temperature and concentration. Using Onsager's (Onsager 1932) reciprocal relations this can be concisely stated as:

$$q = -(-k_T \left(\frac{\partial \mu}{\partial c}\right) i - \kappa \nabla T) \tag{7}$$

$$\mathbf{i} = -\rho(D\nabla c + \frac{Dk_T}{T}\nabla T), \tag{8}$$

where $\kappa = k_T D$. k_T is the thermal diffusion ratio, D the mass diffusion coefficient, μ the difference in the chemical potentials of the two components. κ the thermal conductivity and ρ the density of the mixture (see Landau and Lifshitz 1958, DeGrout and Mazur 1970 and Lee Lucas and Tyler 1983).

If pressure variations were important then the gradient of pressure would appear in equation (8). The inclusion of the terms proportional to ∇T in equation (8) was first recognised to be important by Soret[illegible]. Its inclusion is now commonly refered to as the Soret effect. The converse effect-a flow of heat due to the presence of a concentration gradient is normally refered to as the Dufour effect. The theoretical origins of these effects are discussed in great detail in chapter XI in DeGroot and Mazur (1962). Experimentally the Soret effect is observed to be at least an order of magnitude larger than the Dufour effect (Lucas et al 1983). Consequently, the Dufour effect is largely neglected. Although they are related by Onsager relations the gradient of temperature ∇T is much bigger than ∇c, suitably non-dimensionalised.

In cryogenic $He^3 - He^4$ normal fluid mixtures the Dufour effect can be significant, especially near the thermodynamic tricritical point (Lucas et al 1985). The divergence of several physical quantities near to the thermodynamic tricritical point may be utilised in exploring large regions of

parameter space. In the analysis that follows we shall include the Dufour effect until its inclusion becomes unmanageable. We will discover that the expression for the general binary fluid can be simplified to an uncoupled thermohaline type by a linear change of coordinates, this was first pointed out by Knobloch (1980).

1.3.7 Equations of motion : collated

If we substitute equations (7) and (8) into equations (4) and (5) we obtain:

$$(V.\nabla + \frac{\partial}{\partial t})c = D\nabla^2 c + \frac{Dk_T}{T}\nabla^2 T, \tag{9}$$

$$(V.\nabla + \frac{\partial}{\partial t})T = (D_T + AD)\nabla^2 T + \frac{DTA}{k_T}\nabla^2 c, \tag{10}$$

where $A = k_T^2 \left(\frac{\partial \mu}{\partial c}\right)_{T,p} / TC_p$ is a measure of the Dufour effect. k_T, the thermal diffusion ratio is found to small experimentally. The Dufour effect is of $O(k_T^2)$ and the Soret effect is $O(k_T)$, consequently the Dufour effect is usually neglected. All of the relevant experimental work on binary fluid mixtures has been performed in the absence of an external field causing a significant pressure gradient. This is precisely why equation (10) lacks a term proportional to $\nabla^2 P$ (see Landau and Lifshitz 1958). One would also expect in general that frictional forces would cause internal heating; this we also consider to have negligible effect.

The analysis will concentrate on perturbations from criticality. The subcritical state being characterised by a non-convective, linear temperature

and concentration distribution given by:

$$T = T_0 + \frac{(T - T_0)}{d} z \tag{11}$$

$$c = c_0 + \frac{(c - c_0)}{d} z \tag{12}$$

We may collect together equations (1)-(10) and consider the equations of motion from the motionless quiesent state. We scale time with $\frac{d^2}{D_T}$, velocity with $\frac{D_T}{d}$, temperature with $\frac{\nu D_T}{\alpha g d^3}$ and concentration with $\frac{\nu D_T}{\beta g d^3}$. A natural grouping of parameters occurs for the two-dimensional problem:

$$\Delta(\frac{Dw}{Dt}) = \sigma \Delta^2 w + \sigma \Delta_1(\theta + c), \tag{13}$$

$$\frac{D\theta}{Dt} = \Delta\theta + Rw, \tag{14}$$

$$\frac{Dc}{Dt} = L\Delta c - \psi L \Delta\theta + \psi R w. \tag{15}$$

In writing down equations (13-15) we have chosen to neglect the Dufour effect. w is now the scaled vertical component of velocity, $D_T = \kappa - k_T D$ and θ is chosen interchangably with T. Equation (13) is obtained from the momentum equation. The steps in its derivation are routine. The operator $j.\nabla \times \nabla \times$, which serves to eliminate pressure from the momentum equation, is applied to equation (1). Equation (6) is used to give the equation for the temperature (in rescaled variables the temperature perturbation is θ). The Prandtl number, $\sigma = \frac{\nu}{D_T}$, the Lewis number $L = \frac{D}{D_T} = \frac{1}{\kappa_T}$, the Rayleigh number $R = \frac{g\alpha' \beta d}{\nu D_T}$, ψ is the separation ratio $= \frac{-\beta k_T}{\alpha}$. Δ_2 is the Laplacian, in its two dimensional representation : $\Delta = \frac{\partial^2}{\partial x^2} + \frac{\partial^2}{\partial z^2}$ and $\Delta_1 = \frac{\partial^2}{\partial x^2}$.

1.4 Boundary conditions

It is clear from the subsequent sections that the dynamics of binary fluids are governed by a set of p.d.e.'s involving the dependent variables θ, c and w in a fluid domain D with coordinates (x, z). We must specify what happens at the boundary ∂D. The boundary of the fluid is usually taken to be rigid, suffering no deformation; so the normal component of the velocity field is taken to be zero. The concentration flux, must also vanish on ∂D, indicating no bodily movement of fluid across the boundary-a condition of impermeability. Impermeability and rigidity can be stated concisely as:

$$\theta = i = w = Dw = 0, \qquad z = 0, 1 \tag{16}$$

The linearised version of the equations can be solved for the stationary problem in closed form in terms of hyperbolic functions (see Gutkowitz-Krusin (1979) and in its corrected form by Lucas et al (1983)). The linearised form of equations (13)-(15) have been studied extensively by Schechter et al 1974. The form of the linear solution is straightforward, though laborious to manipulate. Weakly nonlinear theory is rendered hopelessly tiresome if the impervious rigid boundaries are used as a basis for the construction of an amplitude equation.

To circumvent this problem we adopt free slip pervious boundary conditions:

$$\theta = c = w = D^2 w = 0, \qquad z = 0, 1. \tag{17}$$

The 'rigid' condition $Dw = 0$ comes from the fact that u and v, the components of the velocity perpendicular to w are identically zero on the boundary for all x and y. Consequently, using the incompressibility condition $\nabla.V = 0$, $\frac{\partial u}{\partial x} = \frac{\partial v}{\partial y} = 0$ (as u and v are constants on the boundary), and hence $Dw = 0$. For the 'slip' condition $D^2w = 0$, we require the stress tensor to vanish giving $\mu\left(\frac{\partial u}{\partial z} + \frac{\partial w}{\partial x}\right) = 0$. Differentiating the incompressibility condition with respect to z gives the required result $D^2w = 0$.

The conditions in the lateral (x-direction) will be taken to be periodic.

1.5 Symmetries

In a laterally infinite system, laterally periodic boundary conditions may be chosen. In a finite box, the system would no longer be translationally invariant.

We shall assume that the flow has the form of a two-dimensional array of rolls (spatially periodic of period $\frac{2\pi}{k_c}$). An additional requirement, which is supported by the equations themselves, is a reflectional symmetry in any vertical plane. The totality of these symmetries mean that the system possesses $O(2)$ symmetry, the rotations and reflections of the circle. It is the presence of this symmetry that determines the structure of the normal form for a local bifurcation.

1.6 Codimension 2

The reduced system as given by equations (13)-(15) contains two experimentally tunable parameters: the Rayleigh number R, and the separation ratio ψ. The two parameters are independently adjustable. The Rayleigh number is the nondimensionalised version of the temperature difference between the two bounding surfaces. The separation ratio is a nondimensionalised version of the concentration gradient. The separation ratio contains the cross coupling between the temperature and concentration gradients, the thermal expansion coefficient, and the derivative of the density with respect to concentration.

The separation ratio can be made to change sign, for instance, by changing the relative composition of the mixture.

A dynamical system containing two independently adjustable parameters is usually refered to as a two parameter family. Then it is interesting to look for bifurcation phenomena of codimension 1 and 2, since they occur stably in two parameter families. Chapter 2 will clarify its usage.

1.7 Thermohaline, thermosolutal, doubly and multiply diffusive convection

All of the above terms are essentially manifestations of the same phenomena. Thermohaline and thermosolutal convection refer to solutions of salt and solute respectively, in which case the Soret and Dufour effects are ab-

sent. Doubly and multiply diffusive convection are generalisations as they are phenomena that involve two and many diffusive processes respectively.

To be more precise, doubly diffusive convection is generally referred to as convection in a fluid layer with a stabilising concentration gradient.

Examples of experiments are quite diverse. the fluids in question vary from cryogenic $^3He - ^4He$ normal fluid mixtures to alcohol-water systems. The excellent thermal properties of $^3He - ^4He$ (Ahlers 1978) give this pair many advantages over salt-water and ethanol-water systems. The noticeable drawback in the use of low temperature mixtures is that flow visualisation becomes impossible.

1.8 Nusselt number

As it is impractical to visualise the flow in some experiments it is important to have an alternative way of confirming predictions from theory. The heat transported across the fluid layer is one quantity that can be measured and compared with the theory. The appropriate quantity is a non-dimensionalised version of the heat flux called the Nusselt number and is given by:

$$Nu - 1 = \frac{1}{R} \int w\theta dx dz, \tag{18}$$

see Busse (1979) for details.

The disadvantage with this is that it averages out spatial inhomogeneities and hence we receive incomplete information if we wish to in-

vestigate the spatial dynamics of the flow.

Physically, the Nusselt number may be understood as a ratio of conductivities, that is the heat transfered in a convecting state to heat transfered in a conducting state.

Chapter - 2 Dynamical systems theory

2.1 Abstract

The objective of chapter 2 is to gather relevant mathematical material to answer, at least partially, the questions posed in chapter 1. Selection will be made from aspects of dynamical systems theory and reductive perturbation theory.

We must always have in mind: what is the role of dynamical systems in hydrodynamics? This is a difficult and rather technical question to answer in general terms. When the Rayleigh number is small there is a unique correspondence between a given set of boundary conditions and the subsequent flow; this can be proven rigorously by energy methods, see Joseph (1976) for details. When the Rayleigh number increases this uniqueness fails, a multiple solution state is now the rule. Bifurcation theory attempts to provide a substantial mathematical basis for this study.

2.2 Dynamical systems

Dynamical systems theory (D.S.T.) is a diverse and rapidly evolving branch of mathematics. D.S.T. has been used to describe an apparently vast number of phenomena. This is perhaps why it has so much appeal. It has been used, for example, to classify common and universal features in systems as disparate as the Belousov-Zhabotinskii reaction in a stirred flow reactor (Simoyi R.H. 1982) and the Henon map, as the forced simple pendulum

(Kadanoff L 1985) and the phospholipid monolayer (Langer J.S. 1985).

2.3 An overview of dynamical systems

A state of a physical system is information about the system at a given time, that may be contained in a collection of variables. Suppose, for the moment, that the variables $X(t)$ are finite in number $X(t) = (X_1(t), X_2(t), ..., X_n(t))$. The space of states of $X \in U \subset R^n$ is called the phase or state space. Perhaps $X(t)$ is also dependent upon several parameters $\mu = (\mu_1, \mu_2, ..., \mu_p)$. The collection of such μ's is the parameter or control space. When the time evolution of $X(t)$ may be expressed in terms of $X(t)$ and μ , we obtain a system of ordinary differential equations;

$$\frac{dX}{dt} = f(X;\mu), \tag{19}$$

f is appropriately called the vector field, since at each point $(X;\mu)$ we assign a vector $f(X;\mu)$. A solution of (19) together with an initial condition at t=0, is called a trajectory,

$$X(t) = \varphi_t^n(X_0). \tag{20}$$

The collection of mappings;

$$\varphi_t^n : R^n \longrightarrow R^n \tag{21}$$

is a dynamical system. Although, studying the equation governing binary fluids one is not dealing with a dynamical system as described above but we

are dealing with. technically a more difficult object - a semi-flow in infinite dimensions. However. we shall see that much of the interesting behaviour observed in experiments supports the thesis that we may think in terms of low-dimensional systems of equations (Libchaber 1981). This of course skims over many of the technical difficulties in making the transition from the infinite-dimensional system to the finite-dimensional.

2.4 Bifurcation theory

Given a dynamical system, defined by (19), we may wish to understand how qualitative changes in the flow occur as we vary the parameter μ. The variation of the parameters correspond, for example, to adjusting the temperature difference across an experimental cell, or to increasing the available foodstuffs for a species in a population experiment (May 1976). The "basic" state for the convection problem would be the conductive solution in which the fluid is quiesent. In population dynamics the basic state may correspond to the population remaining constant in time. As we change parameters this state may lose stability.

When a loss of stability of the basic state is replaced by a branched or multiple state, resulting in a qualitative change in the flow, we shall call this a bifurcation. In the context of the examples given the new state may be in the form of an oscillating or time periodic state.

We must first address the problem of what do we mean by stability? We take the Lyapunov view of the flow: An equilibrium $\underline{x} = 0$ is stable if

given any $\epsilon > 0$, $\exists$ a $\delta > 0$ such that for every x_0 for which $|x_0| < \delta$. the solution of ψ with initial conditions $\psi(0) = x_0$ can be extended onto all $t > 0$ and satisfies $|\psi(t)| < \epsilon$ for all $t > 0$. This is conveniently pictured in figure 3 and 4 (also see Arnold 1978). The equilibrium is asymptotically stable if it is stable and

$$\lim_{t \to \infty} \psi(t) = 0 \tag{22}$$

There is a useful sufficient condition for asymptotic stability in terms of the eigenvalues of the jacobian matrix $(D_x f)x_0$, defined in Hirsch (1974). The point x_0 is linearly stable if every eigenvalue of $(D_x f)x_0$ has negative real part. It is linearly unstable if at least one eigenvalue has positive real part. Hirsch and Smale 1974, show that x_0 is unstable if it is linearly unstable and asymptotically stable if it is linearly stable. For the degenerate case in which some of the eigenvalues have zero real parts, stability cannot be determined linearly.

The branching process may be conveniently visualised by considering:

$$\{(x, \mu) : f(x, \mu) = 0\}, \tag{23}$$

the graph of x is the bifurcation diagram. The multiplicity of the solution set requires that the matrix $D^u f$ have an eigenvalue 0 (by the implicit function theorem, appendix 4). Otherwise, $det D^u f \neq 0$ gives us a unique solution for x near 0 close to μ_0.

The analysis of bifurcation is performed by studying f near the point of bifurcation and is in this sense referred to as local. It is useful to classify

bifurcations and this may be most effectively done by classifying according to their codimension class. Consistent with Guckenheimer and Holmes 1983 we will use codimension to mean, in this context, the smallest number of parameters which contains the bifurcation in a persistent way. An unfolding of a bifurcation is a family which contains the bifurcation in a persistent way. The concept of unfolding is central to discuss the structural stability of a bifurcation process. Perhaps an example will demonstrate this: the pitchfork bifurcation,

$$\dot{x} = -\mu x + x^3 = f(x,\mu), \qquad \mu = 0. \tag{24}$$

Equation (24) has a bifurcation as μ passes through zero. It is extremely non-robust, in the sense that if we perturb it by changing $f(x,\mu)$ to $\tilde{f}(x,\mu,\mu_\epsilon)$, where $\tilde{f}(x,\mu,\mu_\epsilon) = -\mu x + x^3 + \mu_\epsilon$, there is a drastic change to the bifurcation diagram (see fig. 5). It is important to realise that the introduction of unfolding parameters often corresponds in a physical application to the breaking of some underlying symmetry. The pitchfork example demonstrates how fragile these bifurcations can be. However this bifurcation is persistent in many physical applications. Symmetry forces it to be persistent.

2.5 Centre manifold theory

Centre manifold theory (CMT) gives a beautiful geometrical picture of the flow in phase space (for detailed statements of theorems see Guckenheimer

and Holmes 1983. Carr 1979. and more recently Vanderbauwhede A. 1988). However, because the approach is indirect it is computationally unwieldy as we shall hint at by example.

The behaviour of the solutions to equation (19) is determined by the spectral properties of $Df(0)$. In general we may sub-divide the spectrum of $Df(0)$, call it α, into three distinct parts, namely the stable spectrum $\alpha_s = \{\lambda \epsilon \alpha | \Re(\lambda) < 0\}$, the unstable spectrum $\alpha_u = \{\lambda \epsilon \alpha | \Re(\lambda) > 0\}$, and the centre spectrum $\alpha_c = \{\lambda \epsilon \alpha | \Re(\lambda) = 0\}$. This gives rise to a natural splitting of phase space R^n into invariant subspaces:

$$R^n = X_s \oplus X_u \oplus X_c. \tag{25}$$

Nonzero solutions in the stable subspace X_s decay exponentially, while those in the unstable subspace X_u blow up exponentially. All bounded solutions belong to the centre subspace. The Hartman-Grobman theorem (Guckenheimer and Holmes 1983) states that locally, near $\underline{x} = 0$, the flow of the linearised system and equation (19) are the same via a homeomorphism (provided a non-resonance condition is satisfied), when the centre subspace is empty: in otherwords the singular point $\underline{x} = 0$ is hyperbolic. For non-zero hyperbolic points nonlinear terms in $f(\underline{x})$ will be important. Centre manifold theory serves to prove the existence of invariant manifolds within which the trajectories reside.

Centre manifold theory forms an essential part of dynamical systems. Our concern will be mainly with bifurcation theory, this concentrates on

bounded solutions. such as periodic solutions. The centre manifold contains all such solutions so it seems appropriate to study the flow on such an object.

2.6 Example - the Lorenz model

Recall the Lorenz equations (Lorenz 1963) represent a coupled set of three quadratic differential equations representing three modes (one for the velocity and two for the temperature) of the Oberbeck- Boussinesq equation for fluid convection in a two dimensional layer heated from below. The equations are usually written:

$$\dot{X} = \sigma(Y - X) \tag{26}$$

$$\dot{Y} = \rho X - Y - XZ \tag{27}$$

$$\dot{Z} = -\beta Z + XY \quad \sigma, \rho, \beta > 0, \tag{28}$$

and contain three parameters σ (the Prandtl number), ρ (the Rayleigh number) and β (the aspect ratio). The three mode truncation accurately reflects the dominant convective properties of the fluid for Rayleigh numbers $\rho \simeq 1$. The technique for deriving such a model will be discussed in Chapter 5. The Jacobian derivative at $\underline{0}$ is the matrix:

$$\begin{pmatrix} -\sigma & \sigma & 0 \\ \rho & -1 & 0 \\ 0 & 0 & -\beta \end{pmatrix} \tag{29}$$

When $\rho = 1$, this matrix has eigenvalues 0, $-(1+\sigma)$ and $-\beta$ with eigenvectors $(1,1,0)$, $(\sigma,-1,0)$ and $(0,0,1)$. Using the eigenvalues as a basis for

a new coordinate system, we set

$$\begin{pmatrix} X \\ Y \\ Z \end{pmatrix} = \begin{pmatrix} -\sigma & \sigma & 0 \\ \rho & -1 & 0 \\ 0 & 0 & -\beta \end{pmatrix} \begin{pmatrix} u \\ v \\ w \end{pmatrix}, \tag{30}$$

and hence the inverse transformation is:

$$\begin{pmatrix} u \\ v \\ w \end{pmatrix} = \begin{pmatrix} \frac{1}{1+\sigma} & \frac{\sigma}{1+\sigma} & 0 \\ \frac{1}{1+\sigma} & \frac{-1}{1+\sigma} & 0 \\ 0 & 0 & 1 \end{pmatrix} \begin{pmatrix} X \\ Y \\ Z \end{pmatrix}. \tag{31}$$

Under the transformation given in (30) and (31) the Lorenz equations (26-28) become:

$$\begin{pmatrix} \dot{u} \\ \dot{v} \\ \dot{w} \end{pmatrix} = \begin{pmatrix} 0 & 0 & 0 \\ 0 & (1+\sigma) & 0 \\ 0 & 0 & -\beta \end{pmatrix} \begin{pmatrix} u \\ v \\ w \end{pmatrix} + \begin{pmatrix} \frac{-\sigma}{1+\sigma}(u+\sigma v)w \\ \frac{1}{(1+\sigma)}(u+\sigma v)w \\ (u+\sigma v)(u-v) \end{pmatrix}. \tag{32}$$

To apply C.M.T. we describe the centre manifold as $(v, w) = (h_1(u), h_2(u))$ (Guckenheimer and Holmes 1983) and use the power series method to approximate a centre manifold for the equations up to third order. Hence,

$$\begin{pmatrix} \dot{v} \\ \dot{w} \end{pmatrix} = \begin{pmatrix} (1+\sigma) & 0 \\ 0 & -\beta \end{pmatrix} \begin{pmatrix} v \\ w \end{pmatrix} + \begin{pmatrix} \frac{1}{(1+\sigma)}(u+\sigma v)w \\ (u+\sigma v)(u-v) \end{pmatrix}, \tag{33}$$

making the substitutions $v = h_1(u)$, $u = h_2(u)$ gives:

$$\begin{pmatrix} \dot{h_1}(u) \\ \dot{h_2}(u) \end{pmatrix} \cdot \frac{-\sigma(u+\sigma h_1)h_2}{(1+\sigma)} = \begin{pmatrix} -(1+\sigma)h_1 \\ -\beta h_2 \end{pmatrix} + \tag{34}$$

$$\begin{pmatrix} \frac{1}{(1+\sigma)}(uh_2(u) + \sigma h_1(u)h_2(u))w \\ (u^2 + u(h_1(\sigma-1)) - \sigma h_1^2(u) \end{pmatrix} \tag{35}$$

We make the power series approximation $h_1(u) = a_1u + b_1u^2 + ...$, $h_2(u) = a_2u + b_2u^2 + ...$, this gives

$$-(1+\sigma)(a_1u^2 + b_1u^3 + ...) + \frac{1}{(1+\sigma)}(a_2u^3 + ...) + O(u^4) = 0. \tag{36}$$

By comparing coefficients we find $a_1 = 0$ and $b_1 = \frac{1}{\beta(1+\sigma)^2}$. Hence the dynamics on the centre manifold $h(u) = (h_1(u), h_2(u))$ is given by the amplitude equation:

$$\dot{u} = (-\sigma(\beta(1+\sigma))u^3 + O(u^4). \tag{37}$$

Equations (1) and (2) give an expression for the complete dynamics that go to determine the qualitative behaviour of the Lorenz equations at $\rho = 1$. This static problem gives us very little information about the dynamics of the system other than at $\rho = 1$. We wish to approximate the centre manifold $(u, w) = (h_1(u, \rho),\ h_2(u, \rho))$ for the Lorenz equations when ρ is close to 1. To do this we use the same transformation as given in equation (30) except keep ρ as a variable parameter. Carrying out this proceedure yields:

$$\begin{pmatrix} \dot{u} \\ \dot{v} \\ \dot{w} \end{pmatrix} = \begin{pmatrix} 0 & 0 & 0 \\ 0 & (1+\sigma) & 0 \\ 0 & 0 & -\beta \end{pmatrix} \begin{pmatrix} u \\ v \\ w \end{pmatrix} + \tag{38}$$

$$\begin{pmatrix} \frac{-\sigma}{1+\sigma}(u+\sigma v)w \\ \frac{1}{(1+\sigma)}(u+\sigma v)w \\ (u+\sigma v)(u-v) \end{pmatrix} + \begin{pmatrix} \frac{\rho_1\sigma}{(1+\sigma)} & \frac{\rho_1\sigma^2}{(1+\sigma)} & 0 \\ -\frac{\rho_1}{(1+\sigma)} & -\frac{\rho_1\sigma}{(1+\sigma)} & 0 \\ 0 & 0 & 0 \end{pmatrix} \begin{pmatrix} u \\ v \\ w \end{pmatrix}, \quad \rho = 1+\rho_1. \tag{39}$$

We seek a centre manifold that is a homogeneous polynomial of the variables of the centre manifold, ρ_1 and u. Hence, choosing

$$h_1(u, \rho_1) = a_1u^2 + b_1u\rho_1 + c_1\rho_1^2 + O(3), \tag{40}$$

$$h_2(u, \rho_1) = a_2u^2 + b_2u\rho_1 + c_2\rho_1^2 + O(3), \tag{41}$$

by substituiton of the power series (40) and (41) and comparing coefficients we obtain:

$$\dot{u} = \frac{\rho_1\sigma}{(1+\sigma)}\left(1 - \frac{\sigma\rho_1}{(1+\sigma)}\right)u - \frac{\sigma}{(1+\sigma)\beta}\left(\frac{\sigma\rho_1}{(1+\sigma)^2} - 1\right)u^3. \qquad (42)$$

Equation (42) describes the dynamics in the centre manifold.

2.7 Reductive perturbation theory

As an alternative to centre manifold theory, reductive perturbation theory or the method of multiple scales provides a substantial method of deriving amplitude equations. The first step in performing reductive perturbation theory is, as in the centre manifold approach, to identify the eigenvalues. We expand around $\rho = 1$. For $\rho < 1$ we know from Hartman's theorem that the sero solution is stable. We expand in a small parameter ϵ:

$$(X, Y, Z) = \epsilon(X_1, Y_1, Z_1) + \epsilon^2(X_2, Y_2, Z_2) + ... \qquad (43)$$

also,

$$\rho = 1 + \epsilon\rho_1 + \epsilon^2\rho_2 + ..., \qquad (44)$$

and by introducing many time scales $\tau_0 = t$, $\tau_1 = \epsilon t$, $\tau_2 = \epsilon^2 t$, ... we have to lowest order

$$D_0\underline{\dot{X}}_1 = \begin{pmatrix} -\sigma & \sigma & 0 \\ \rho_1 & -1 & 0 \\ 0 & 0 & -\beta \end{pmatrix}\begin{pmatrix} X_1 \\ Y_1 \\ Z_1 \end{pmatrix} = L\underline{X}_1, \qquad (45)$$

where $D_0 = \frac{\partial}{\partial\tau_0}$, $D_1 = \epsilon\frac{\partial}{\partial\tau_1}$, ... For $\rho = 1$ the stationary solution requires X_1 to be independent of τ_1. The eigenvector of L corresponding to $\rho_1 = 1$ is $(X_1, Y_1, Z_1)^T = (1.1, 0)$.

To $O(\epsilon^2)$,

$$D_0\underline{X}_2 + D_1\underline{X}_1 = L\underline{X}_2 + \begin{pmatrix} 0 \\ 0 \\ X_1Y_1 \end{pmatrix} \tag{46}$$

$$D_1\underline{X}_1 = L\underline{X}_2 + \begin{pmatrix} 0 \\ 0 \\ X_1^2 \end{pmatrix} + \begin{pmatrix} 0 \\ \rho_2 X_1 \\ 0 \end{pmatrix} \tag{47}$$

with adjoint or left eigenvector $(\bar{X}_1, \bar{Y}_1, Z_1) = (1, \sigma, 0)$. The solvability condition requires (see Nayfeh and Mook 1973)

$$-(D_1X_1 + \sigma D_1Y_1) + \sigma\rho_2 X_1 = 0. \tag{48}$$

A sufficient condition for solvability is that X_1 be independent of τ_1 and $\rho_2 = 0$. Solving to second order requires $X_2 = X_1 = Y_2$, $Z_2 = \frac{X_1^2}{\beta}$.

To $O(\epsilon^3)$,

$$D_2\underline{X}_1 = L\underline{X}_3 + \begin{pmatrix} 0 \\ \rho_3 X_1 \\ 0 \end{pmatrix} + \begin{pmatrix} 0 \\ X_1 Z_2 \\ 0 \end{pmatrix}. \tag{49}$$

This gives the solvability condition found from equation (49) by multiplying by the adjoint derived from equation (45):

$$\frac{(1+\sigma)}{\sigma} D_2X_1 = \rho_3 X_1 + \frac{X_1^3}{\beta}. \tag{50}$$

Finally,

$$\frac{\partial X_1}{\partial \tau_2} = \frac{\sigma}{(1+\sigma)}(\rho - \rho_1)X_1 + \frac{\sigma}{(1+\sigma)\beta} X_1^3, \tag{51}$$

the required form of the amplitude equation.

The Lorenz example serves to demonstrate the two techniques, in systems of model equations that we shall subsequently study the reductive

perturbative approach will prove to be more efficient in the derivation of the amplitude equations. Details of the techniques are given in two excellent books, Guckenheimer and Holmes 1983 for the centre manifold theory and Nayfeh and Mook 1973 for the perturbative approach.

2.8 Hopf bifurcation

There are many bifurcations that warrant discussion, perhaps the most important we shall encounter, in the context of convection in binary fluids is the Hopf bifurcation. The theorem of Hopf we state is taken from Marsden and McCracken 1975 and is due primarily to Hopf 1932 (also Poincare and Andronov).

It states:

Theorem: Hopf bifurcation theorem for vector fields

Let X_μ be a $C^k(k > 4)$ vector field on R^2 such that $X_\mu = 0$ for all μ. Let $DX_\mu(0,0)$ have distinct, simple complex conjugate eigenvalues $\lambda(\mu)$ and $\overline{\lambda(\mu)}$ such that for $\mu = 0$, $\Re(\lambda) = 0$. Assume $\frac{d\Re(\lambda(\mu))}{d\mu}|_{\mu=0} > 0$. Then there is a C^{k-2} function $\mu : (-\epsilon, \epsilon) \longrightarrow R$ such that $(X_1, 0, \mu(X_1))$ is on a closed orbit of period $\approx \frac{2\pi}{|\lambda(0)|}$ and radius growing like $\sqrt{\mu}$, of the flow of X for $X_1 \neq 0$ and such that $\mu(0) = 0$.

A Hopf bifurcation is observed in the Lorenz system at parameter values $(\rho, \sigma, \beta) = (24.7, 10, \frac{8}{3})$ (Sparrow 1983).

2.9 Application of Lie groups

Bifurcations, associated with the qualitative change in fluid flow, provides fertile ground for the study of pattern selection. The presence of a continuous symmetry (a Lie group), forced through the presence of internal and boundary constraints, has a remarkable effect on the expected dynamics.

From a mathematical point of view symmetry often increases the multiplicity of the eigenspectrum whilst decreasing the complexity of the nonlinearities allowed (Olver 1982). The Hopf bifurcation in the presence of symmetry has been in a state of vigorous study both from a reductive perturbative viewpoint (Knobloch 1985) and from a more formal approach by using equivariant bifurcation theory. In the presence of $O(2)$ symmetry a number of interesting phenomena have been observed. Golubitsky and Stewart 1985 rederive the generalised form of Hopf theorem. A few definitions must be made before the theorem of Hopf can be stated.

Definition: Γ denotes the group of symmetries of the set of O.D.E.'s of equation (19).

Definition: The symmetries of a steady state solution form a sub group of Γ, is called the isotropy subgroup of that solution.

Definition: The periodic solution $X(t)$ has a spatial symmetry $\gamma \in \Gamma$ if for every t, $\gamma X(t) = X(t)$.

Theorem: Let Σ be an isotropy subgroup of Γ such that the fixed point

subspace $\mathrm{Fix}(\Sigma)$ is two-dimensional. Assume that $Df(0)$ is such that

$$Df(0) = \begin{pmatrix} aI & bI \\ cI & dI \end{pmatrix}, \tag{52}$$

together with the usual transversality condition on the eigenvalues. Then there is a unique branch of small amplitude periodic solutions to equation (19) , of period near 2π, whose spatial symmetries are Σ.

2.10 Hopf with symmetry

Symmetry also aids in the simplification of the nonlinearities that are important. The basis of the method we shall use, called equivarient bifurcation theory is best explained by example. Assume for the moment that the stream function of a purely 2-D flow may be represented by a superposition of left and right travelling waves

$$\psi(x,z;t) = [(v+w)e^{i\omega_0 t} + (\overline{v}+\overline{w})e^{-i\omega_0 t}]\sin\pi z. \tag{53}$$

The condition $v = \overline{w}$ gives a stationary wave.

Here,

$$\dot{v} = i\omega_0 v \tag{54}$$

$$\dot{w} = -i\omega_0 w \tag{55}$$

where v and w are the complex amplitudes of the left and right travelling waves. In the presence of $O(2)$ symmetry - the symmetry of the circle under reflections and rotations (occuring naturally in the Binary fluid convection

problem because of the spatial periodicity of the rolls) then there are three invariants of the motion

$$\sigma_1 = v\bar{v} + w\bar{w} \tag{56}$$

$$\sigma_2 = v\bar{w} \tag{57}$$

$$\sigma_3 = \bar{v}w \tag{58}$$

If we construct the vector field from the above invariants then the vector field will be equivariant under these symmetry operations (see Chapter 4).

An additional symmetry that arises in the Hopf bifurcation $S(1)$ is the phase shift symmetry - this being due to the temporal symmetry due to the periodic nature of limit cycle (a time shift of τ, $t \longrightarrow t + \tau$, takes you back to the same place.

2.11 Extensions to the finite dimensional Centre Manifold theory

Although the theorem stated in section (2.7) is finite dimensional there are possible generalisations. The assumptions that the eigenvalues of the linearised problem all have non-positive real parts is not necessary (Carr 1979). The equations also need not be autonomous.

It has been attempted in this chapter to give a overview of dynamical systems. Many, many aspects of the theory have been omitted. It still remains an open question to what degree it has to play in hydrodynamics. However. the prospects look very promising.

Chapter 3 - Tricritical bifurcation

3.1 Introduction to the tricritical bifurcation

For a vector field f with reflectional symmetry we say that it has Z_2 symmetry. This terminology is used because the two element group $Z_2 = \{1, R\}$ acts on the real line, where 1 is the identity and $Rx = -x$ is the reflection operator. Bifurcations of this type arise often in physical applications. The effect of this symmetry group on a bifurcation in binary fluid convection will be explored. In this context the presence of Z_2 symmetry implies the presence of up-down reflectional symmetry of the convective rolls.

Z_2 makes all the terms in the stationary bifurcation odd. We may expect to use equivariant bifurcation theory to the model problem. We then expect to express the stationary codimension 1 problem as an expansion, assuming the vector field f to be sufficiently smooth:

$$\frac{dA}{dt} = f(\mu, A^2)A, \tag{59}$$

where μ is a bifurcation parameter. For small amplitude A we may expect to be able to expand f as an equivariant Taylor series , i.e. a Taylor series that is invariant under the symmetry group. It will be the purpose of the beginning of this chapter to outline basic results we can expect, based upon general considerations from equivariant bifurcation theory. Returning to equation (59), the expanded version takes on the form:

$$\frac{dA}{dt} = (\lambda - \alpha_1 A^2 - \alpha_2 A^4, ...)A. \tag{60}$$

To $O(A^3)$ the amplitude equation describes the usual pitchfork (bifurcation) provided $\alpha_1 < 0$ see fig(2). In non-generic circumstances, or owing to the presence of some physical constraint, in which $\alpha_2 > 0$ the term $O(A^5)$ is needed if the bifurcation is to be forward and supercritical. Clearly, if $\alpha_3, \alpha_4, etc. > 0$ then we cannot hope to describe the instability in terms of a small amplitude expansion (in a local sense).

We consider, for the moment, equation (3.1) retaining terms up to $O(A^5)$ with the coefficient of A^5 normalised. We expect the stationary bifurcation to differ from the usual pitchfork bifurcation, by Ahlers (1980). This is perhaps most easily visualised via the bifurcation diagrams depicted in fig 6, where the solid line denotes a stable branch and the broken line is an unstable branch. This bifurcation has been recently christened the tricritical bifurcation. The experimental verification of this bifurcation has been the subject of some controversy in the literature (Ahlers (1986), Gao and Rehdberg(1986)). We will address ourselves to the tricritical bifurcation, in detail, in this chapter.

3.2 The mechanical analogue

A simple mechanical analogue of the tricritical bifurcation was given by Benjamin (see Joseph(1977)). Consider an arch of wire passed through a rigid board, buckling of the wire is observed as the length of wire, l is increased see Fig(6). This buckling may occur with equal probability to the left or right assuming exact symmetry.

When l is small, the arch of wire remains upright. the angle measured from the vertical, $\theta = 0$ is stable. The solution $\theta = 0$ becomes unstable when the wire reaches a critical length, l_c, where upon the wire flops to a value θ_c. As the wire is shortened it remains in the symmetry broken state until a point l_h is reached where the wire flips back to the symmetric upright position. This example shows hysteresis, characteristic of the tricritical bifurcation.

3.3 Linear theory

When the amplitude of convection is small enough that the advective terms $\vec{V}.\vec{\nabla}\vec{V}$, $\vec{V}.\vec{\nabla}\theta$ and $\vec{V}.\nabla c$ can be neglected, equations (1.5-1.7) become linear. The instability of the static or conductive layer occur in the form of monotonically (exponentially) growing disturbances. The analysis of convection near marginal stability can be restricted to the time-independent problem (for the single fluid); this is generally known classically as the "principle of exchange of stabilities" (Chandrasekar 1954).

The usual stability problem associated with equations (13-15) together with the boundary conditions (17) is to find the smallest temperature gradient which allows undamped solutions of the linearised equations. In the free-free (both bounding surfaces free slip), pervious perfectly conducting boundary situation a disturbance of the form

$$exp(i\vec{k}.\vec{x})sin(\frac{m\pi z}{d}), \tag{61}$$

will be a solution at criticality. It becomes unstable for $R > R_c$, where R_c is a critical value of the Rayleigh number.

3.4 Critical Rayleigh number with idealised boundaries

The linear operator Λ associated with the linearisation of equation(13-15) of chapter 1 is:

$$\Lambda = \begin{pmatrix} \Delta^2 & (1+\psi)\partial_{xx} & -\psi\partial_{xx} \\ R & \Delta & L\Lambda\Delta \\ 0 & \Delta & L(1+\Lambda)\Delta \end{pmatrix}, \tag{62}$$

with $\vec{w_0} = (w_0, \theta_0, x_{i_0})$, where $\Delta = \partial_{xx} + \partial_{zz}$ is the two dimensional Laplacian. The vector $\vec{w_0}$ is periodic in both x and z, that is, $\vec{w_0} \propto \vec{w_0} \sin k_z z \cos k_x x$. This in turn gives the matrix equation $\Lambda\vec{w_0} = L\vec{w_0} = 0$. The critical Rayleigh number is determined from the condition for non-trivial solvability, $det(L) = 0$. This gives when the periodic ansatz (61) is substituted into equation (62):

$$R_c = \frac{k^6}{k_x^2((1+\psi)(1+\Lambda)+\frac{\psi}{L})}. \tag{63}$$

We may represent this stability relation graphically. By fixing ψ, Λ and L the critical wave number which will become unstable is $k_m = \frac{\pi}{\sqrt{2}}$, (found by calculating $\frac{dR_c}{dk_x^2}$), $k_z = \pi$ and gives,

$$R_c = \frac{27\pi^4}{4((1+\psi)(1+\Lambda)+\frac{\psi}{L})}. \tag{64}$$

3.5 Linear theory with realistic boundaries

In experiments, the above boundary conditions are unrealistic. The boundaries are rigid and impervious. However, away from the boundary layer for the rigid case we could possibly expect a situation that simulates the free-slip case. The linear theory for the more realistic boundaries have been treated by Hurle and Jakeman (1970), and subsequently by others, numerically. The stability diagram for the rigid impervious case has the same features as for the free, pervious case, except that the critical Rayleigh number is a factor of 2.1 times smaller than in the rigid case. Pseudo- variational techniques (Schecter et al 1970) have been used to circumvent unnecessary calculation in the Hopf bifurcation observed in linear theory. Linear theory utilising experimentally realistic boundary conditions accurately predicts conditions for onset of convection(Lee, Lucas and Tyler 1983). However, expanding about such a solution, as one would when using a weakly nonlinear perturbative approach, is tedious. In a sense it is also unrewarding, for the expansion using the simplified boundary conditions is straightforward and yet it yields qualitatively the correct results.

3.6 The ϵ hierarchy

The basic strategy, involved in deriving an amplitude equation of the form of (3.1) directly from the P.D.E.'s (equations (1.5-1.9)), is to solve, perturbatively, the weakly non-linear problem, associated with choosing a Rayleigh

number close to criticality. The amplitude equation then results when we demand the expansion to be consistent. This process is not as inexact as many have made it out to be (for criticisms see Holmes 1977 on the virtues of centre manifold theory versus perturbative methods).

The linearisation, $L w_0 = 0$ is an eigenvalue problem that involves two independently chosen parameters R and ψ. The Rayleigh number, R, may then be chosen to assume a critical value, R_c, forcing a one-dimensional centre manifold (see section 2.4). If R is chosen to be exactly R_c, then it is clear from the stability diagram, fig 9, that the binary fluid system selects uniquely a horizontal wavelength. With horizontal walls this assertion can be false. This was demonstrated most strikingly in the Taylor-Couette system (Benjamin and Mullin 1980) in which given a fixed speed of rotation many different kinds of flow can be realised, each depending upon how the system is started up. Taking into consideration these possibilities it is our intention to expand about this linearly unstable state as R is chosen to be marginally greater than R_c.

We expand the variables $\tilde{V}$, T, c and the parameter about the critical state in the form of a power series in a small dimensionless parameter ϵ, where, intuitively ϵ may be regarded as a measure of the strength of the convection. The velocity we write as:

$$\tilde{V} = (\epsilon u_1 + \epsilon^2 u_2 + \ldots, \epsilon w_1 + \epsilon^2 w_2 + \ldots), \qquad (65)$$

the basic state we recall is the stationary state given by $\tilde{V} = 0$. The

temperature we write as:

$$\theta = \theta_0 + \epsilon\theta_1 + \epsilon^2\theta_2 + \ldots\ldots, \tag{66}$$

similarly the concentration we express as:

$$c = c_0 + \epsilon c_1 + \epsilon^2 c_2 + \ldots\ldots \tag{67}$$

where θ_0 and c_0 are the linear solutions of equations (11) and (12). Also, we may wish to expand, in a similar fashion to the temporal scale the spatial scales. The reason for such an expansion is that we may have a slow spatial modulation of the basic purely 2-D roll state. A source of spatial modulation is the forcing induced by the presence of side walls (Segal 1969). Assuming a continuous band width of modes about criticality we may obtain a Newell-Whitehead type of equation (1969). This possibility is explored later. For the moment we restrict ourselves to the temporal problem. We express the time, t in terms of new independent variables, commonly referred to as slow times according to:

$$\tau_n = \epsilon^n t, \tag{68}$$

for $n = 0, 1, 2, \ldots$. It follows that the first derivative with respect to t becomes an expansion in terms of the partial derivatives with respect to the τ's:

$$\begin{aligned} \frac{d}{dt} &= \frac{\partial \tau_0}{\partial t}\frac{\partial}{\partial \tau_0} + \frac{\partial \tau_1}{\partial t}\frac{\partial}{\partial \tau_1} + \ldots. \\ &= \frac{\partial}{\partial \tau_0} + \epsilon\frac{\partial}{\partial \tau_1} + \ldots. \end{aligned} \tag{69}$$

One assumes u_1, w_1, θ_1 and c_1 are functions of τ_0, τ_1.....etc. We expect the number of independent time scales to depend upon the order we wish to take the expansion.

3.7 $O(\epsilon)$

We substitute all of the expansions given by the relations $(65-69)$ into the basic equations and we equate powers of ϵ, to $O(\epsilon)$ we find:

$$\begin{pmatrix} \Delta^2 & (1+w)\partial_{zz} & -w\partial_{zz} \\ R & \Delta & LA\Delta \\ 0 & \Delta & L(1+A)\Delta \end{pmatrix} \begin{pmatrix} w_0 \\ \alpha \\ \beta \end{pmatrix} = \begin{pmatrix} \frac{-1}{P}k^2\frac{\partial w_0}{\partial \tau_0} \\ \frac{\partial \alpha}{\partial \tau_0} \\ \frac{\partial \beta}{\partial \tau_0} \end{pmatrix} \tag{70}$$

For $R = R_c$, w_0 is independent of τ_0, hence the R.H.S. of (70) is identically zero. We have, of course, assumed the ansatz:

$$\vec{w_0} = \begin{pmatrix} 1 \\ \alpha \\ \beta \end{pmatrix} sin\pi z cosk_c x, \tag{71}$$

assuming the horizontal wave number, k_c takes the critical value at $k_{c_c} = \frac{\pi}{\sqrt{2}}$. The eigenvalue problem posed by equation (70) is solved by choosing $\alpha = \frac{(1+A)R_c}{\pi^2}$ and $\beta = \frac{AR_c}{L\pi^2}$. The undetermined multiplier w_0 is called the amplitude of convection. In the subsequent analysis we derive an amplitude equation describing the temporal evolution of w_0.

For sake of brevity S will denote the sine function and C the cosine function. This will serve to condense some of the algebra. Proceeding to second order in ϵ requires contributions from the advective terms. The advective nonlinearity in equation (13) vanishes identically in the case of

periodic boundary conditions. For terms of the form $w_p = C(\alpha x)S(\beta z)$, incompressibility requires $u_p = -\frac{\beta}{\alpha}S(\alpha x)C(\beta z)$. Substitution of these two expressions for w_p and u_p into the nonlinearity $w\nabla u - u\nabla w$ gives the required result:

$$w\nabla u - u\nabla w = 0. \tag{72}$$

3.8 $0(\epsilon^2)$

To second order in ϵ we encounter an equation of the form:

$$Lw(R_c) = \begin{pmatrix} 0 \\ \alpha_1 \\ \beta_1 \end{pmatrix} S(2k_c z) + \frac{w_0 k_c}{2} \begin{pmatrix} \frac{\partial w_1}{\partial \tau_1} \\ \frac{\partial \theta_1}{\partial \tau_1} \\ \frac{\partial \bar{V}_1}{\partial \tau_1} \\ \frac{\partial c_1}{\partial \tau_1} \end{pmatrix} C(k_c x)S(k_c z), \tag{73}$$

where $\vec{w}_1 = \frac{\partial w_1}{w_0 k_c}$. We notice that the second term on the right hand side resonates with the eigenvector associated with the linear operator L. We may rescale time and the Rayleigh number to remove this secularity. For consistency we require R_1 and the variables $\bar{V}$, θ and c be independent of τ_1. We have therefore eliminated the second term on the right hand side of equation (13) completely, avoiding any resonant behaviour. We express $\vec{w}_1$ as follows:

$$\vec{w}_1 = \begin{pmatrix} 0 \\ \alpha_2 \\ \beta_2 \end{pmatrix} S(2k_c z), \tag{74}$$

this gives:

$$\begin{pmatrix} -(2k_c)^2\alpha_2 & -LA(2k_c)^2\beta_2 \\ -(2k_c)^2\alpha_2 & -L(1-A)(2k_c)^2\beta_2 \end{pmatrix} = \begin{pmatrix} \alpha_1 \\ \beta_1 \end{pmatrix} \tag{75}$$

We solve for α_2 and β_2:

$$\alpha_2 = \frac{-1}{(2k_z)^2}((1+A)\alpha - A\beta), \tag{76}$$

$$\beta_2 = \frac{1}{(2k_z)^2 L}(\alpha - \beta) \tag{77}$$

A third equation does not appear in the two dimensional equation (75) since the ansatz is independent of x. Reexpressing in terms of the original variables gives:

$$w_1 = \frac{R_a w_0^2}{8k^2 k_z} \begin{pmatrix} 0 \\ -(\frac{A}{L} + (1+A)^2) \\ \frac{1}{L}(1 + A + \frac{1}{L}) \end{pmatrix} S(2k_z z). \tag{78}$$

3.9 $0(\epsilon^3)$

We proceed iteratively. To order $0(\epsilon^3)$ we need to calculate all the contributions from the advective terms. However, w_1 is independent of x, hence only terms of the form $w_0 \partial_z w_1$ will be needed.

We obtain,

$$Lw_2 = \begin{pmatrix} 0 \\ p \\ q \end{pmatrix} (S(3k_z z) - S(k_z z))C(k_z z) + \begin{pmatrix} \frac{-1}{2} k^2 \frac{\partial p_{33}}{\partial z} \\ \frac{\partial p_{23}}{\partial z} \\ \frac{\partial p_{33}}{\partial z} \end{pmatrix}, \tag{79}$$

with

$$p = \frac{-w_0^2 R_a}{8k^2} \left(\frac{A}{L} + (1+A)^2 \right) \tag{80}$$

$$q = \frac{w_0^2 R_a}{8k^2 L} \left(1 - A + \frac{1}{L} \right). \tag{81}$$

Clearly, we cannot rescale at this order to remove secular contributions. The solvability conditions require that the inhomogeneous part of

each equation to be orthogonal to the homogeneous solution of the adjoint operator $L^{\dagger}$, associated with the linear operator L. The adjoint is defined by the relation:

$$w_0^{\dagger} L w_0 = w_0 L^{\dagger} w_0^{\dagger} \tag{82}$$

A recipe for deriving $w_0^{\dagger}$, or the left eigenvector of L utilises integration by parts, see Roberts (1960). The equations in this matrix form are algebraic and hence the above condition reduces to multiplying the left eigenvector by a constant matrix, and equating to zero. The row vector $(w^{\dagger}, \theta^{\dagger}, c^{\dagger})$ denotes the left eigenvector. The consistency condition may be concisely written as:

$$(w^{\dagger}, \theta^{\dagger}, c^{\dagger}) \begin{pmatrix} k^4 & -(1-\psi)k_x^2 & \psi k_x^2 \\ R & -k^2 & -LAk^2 \\ 0 & -k^2 & -L(1+A)k^2 \end{pmatrix} \begin{pmatrix} w \\ \theta \\ c \end{pmatrix} = 0, \tag{83}$$

we rearrange this to give:

$$(w, \theta, c) \begin{pmatrix} k^4 & R & 0 \\ -(1+\psi)k_x^2 & -k^2 & -k^2 \\ \psi k_x^2 & -LAk^2 & -L(1+A)k^2 \end{pmatrix} \begin{pmatrix} w^{\dagger} \\ \theta^{\dagger} \\ c^{\dagger} \end{pmatrix} = 0, \tag{84}$$

Hence, the left eigenvector is;

$$\vec{w_0^{\dagger}} = \begin{pmatrix} 1 \\ \frac{-k^4}{R} \\ -(1+\psi)\frac{k_x^2}{k^2} + \frac{k_x^2}{R} \end{pmatrix} \tag{85}$$

The prescription for consistency demands multiplication on the left of those terms proportional to $S(k_x x)C(k_z z)$. This procedure gives:

$$\left(\frac{-1}{P} k^2 \frac{\partial w_0}{\partial \tau} - R_T w_0\right) \cdot 1 - \left(\frac{\partial \theta_0}{\partial \tau} - p\right) \cdot \frac{-k^4}{R} \tag{86}$$

$$\left(-(1-\psi)\frac{k_x^2}{k^2}-\frac{k^4}{R}\right)\left(\frac{\partial \dot{w}_0}{\partial r}-q\right)=0 \tag{87}$$

rearranging and simplifying yields:

$$\Delta\frac{\partial w_0}{\partial r}-\alpha w_0-\beta w_0^2=0 \tag{88}$$

where the constants are defined as,

$$\alpha=\frac{R_2}{\alpha_1} \tag{89}$$

$$\beta=\frac{-k^2}{8\alpha_1}\left((1+\psi)(1+A)+\frac{\psi}{L}\right) \tag{90}$$

$$\Delta = (1+A)^3+\frac{2(1+A)A}{L}+\frac{A}{L^2} \tag{91}$$

$$+\ \psi\left(1+A+\frac{1}{L}\right)\left((1+A)^2\frac{2A}{L}+\frac{1}{L^2}\right) \tag{92}$$

We notice that β can assume either sign according to the choice of separation ratio, ψ. The coefficient β vanishes identically when:

$$\psi_t=-\frac{\left((1+A)^3+\frac{2(1+A)A}{L}+\frac{A}{L^2}\right)}{\left(1+A+\frac{1}{L}\right)\left((1+A)^2+\frac{2A}{L}+\frac{1}{L^2}\right)}, \tag{93}$$

We may therefore conclude that no small amplitude description exist at this order for $0>\psi>\psi_t$.

To seek a higher order amplitude equation we must obviously take the perturbative expansion to higher order in ϵ. However, ordering $R-R_c\sim 0(\epsilon^2)$ and $t=\epsilon^2\tau_2\sim 0(\epsilon^2)$ is inadequate, in as much as it brings in linear

and time dependent terms too early; this can be easily remedied by altering the ordering to:

$$R - R_c \sim 0(\epsilon^4), \quad t = \epsilon^4 \tau_4 \sim 0(\epsilon^4), \quad \psi - \psi_c \sim 0(\epsilon^2). \tag{94}$$

This new ordering will result in all terms of the amplitude equation of the same order. The procedure of generating and solving the ϵ- hierarchy is continued. Recall equation (79), we must solve, at third order, for terms proportional to $S(3k_c z)C(k_c z)$. We assume a solution to third order of the form:

$$\vec{w_3} = \begin{pmatrix} \delta_1 \\ \delta_2 \\ \delta_3 \end{pmatrix} S(3k_c z)C(k_c z), \tag{95}$$

this results in;

$$\begin{pmatrix} k_\phi^4 & -(1+\psi)k_\phi^2 & k_\phi^2 \\ R & -k_\phi^2 & -LAk_\phi^2 \\ 0 & -k_\phi^2 & -L(1+A) \end{pmatrix} \begin{pmatrix} \delta_1 \\ \delta_2 \\ \delta_3 \end{pmatrix} = \begin{pmatrix} 0 \\ p \\ q \end{pmatrix}, \tag{96}$$

where $k_\phi^2 = ((3k_c)^2 + k_m^2)$. Already, expressions for $\delta_1, \delta_2, \delta_3$ are beginning to become unwieldy. We make the reasonable approximation that the Dufour effect is negligibly small, or $A = 0$; this results in a considerable simplification. We evaluate $\delta_1, \delta_2, \delta_3$ at $\psi = \psi_c$; this gives

$$\delta_1 = 0, \quad \delta_2 = \frac{w_0 R_c}{81\epsilon^2 k_\phi^2}, \quad \delta_3 = \frac{-w_0 R_c(1+L+L^2)}{81k^2 k_m^2 L^2}. \tag{97}$$

3.10 $0(\epsilon^4)$

The fourth order contributions are of the following form:

$$w_0 \partial_- \theta_3 + u_0 \partial_x \theta_3, \qquad w_0 \partial_z \zeta_3 - u_0 \partial_0 \zeta_3. \tag{98}$$

We use trigonometrical identities, given in appendix(4) to simplify equation(97). We are then faced with an equation of the form:

$$Lw_3 = \frac{w_0^4 R_c k_z}{32k^2 k_\phi^2} \begin{pmatrix} 0 \\ -1 \\ \frac{(1+L+L^2)}{L^2} \end{pmatrix} (4S(4k_z) - 2S(2k_z) + 2C(2k_z z) + ...) \quad (99)$$

Our interest will be primarily focused on the mechanics of the derivation of the amplitude equation. We can save unnecessary calculation by realising, at this stage, that not all of the terms in equation (98) are essential. As we found at second order the terms proportional to $S(2k_z)$ contributed. Solving for the terms in equation(98) proportional to $S(2k_z)$ gives:

$$\begin{pmatrix} 0 \\ 1 \\ -\frac{(1+L+L^2+L^3)}{L^3} \end{pmatrix} \frac{w_0^4 R_c}{64k^2 k_\phi^2 \ k_z} S(2k_z z). \quad (100)$$

3.11 The amplitude equation

To derive the amplitude equation at third order we do not need to solve at third order, but only to derive the consistency condition. The consistency condition is determined from the potentially secular terms. In an analogous fashion we derive the amplitude equation at fifth order. We multiply on the left by $w_0^\dagger$ to derive the consistency condition:

$$\frac{dw_0}{d\tau} = \alpha w_0 - \beta w_0^3 + \gamma w_0^5. \quad (101)$$

The constants appearing in the above expression are:

$$\alpha = \frac{k^2(R - R_c)}{\chi R_c} \quad (102)$$

$$\beta = \frac{(\psi - \psi_c)R_c k_c^2(1 - A - \frac{1}{L})(\frac{2A}{L} - (1 - A)^2 - \frac{1}{L^2})}{8\chi k^4} \tag{103}$$

$$\gamma = \frac{-1}{64k_c^6 \quad L^2\chi} \tag{104}$$

$$\chi = \frac{1}{\sigma} - 1 + A + \frac{k_c^2 R_c}{Lk^4}(\psi_c(A - \frac{1}{L}) + A) \tag{105}$$

3.12 Calculation of the Nusselt number

What conclusions can we draw from equation (101). An immediate consequence of the relation(100) is that for $R > R_c$ and $\psi > \psi_t$ we have the sought-after fifth order saturation of the linearly unstable mode, since $L > 0$. We use the saturated amplitude:

$$Nu - 1 = \frac{1}{R}\int w\theta dxdz. \tag{106}$$

We can evaluate the Nusselt number in the various regions of criticality; subcritical, tricritical, and supercritical. This is most easily achieved by evaluation of equation (106) to lowest order ($w = w_0, \theta = \theta_0$). The integrals are trivial.

$$w_0^2 = \begin{cases} \frac{\alpha}{\beta} & \psi > \psi_t \\ \sqrt{\frac{\alpha}{\gamma}} & \psi = \psi t \\ \beta \pm \frac{\sqrt{\beta^2 - 4\gamma\alpha}}{2\gamma} & \psi > \psi t \end{cases} \tag{107}$$

3.13 Experimental evidence

There is tentative experimental evidence for the tricritical bifurcation. Gao and Behringer (1986) perform their experiment on a $He^3 - He^4$ normal fluid

mixtureϕ. The nature of the fluid prevents a direct observation of the flow. A series of Nusselt plots from the experiment of Gao and Behringer (1986) are of the form:

$$Nu - 1 = C_1\sqrt{\frac{(R - R_c)}{R_c}}, \tag{108}$$

but the values of ψ are too few to make a firm connection between theory and experiment. For L = 0.04, A = 0, values appropriate to the experiment of Gao and Behringer, we obtain a value of $C_{1-th} = 0.2$. Their experimental results, fitted to a curve of the form of equation (107), give a value of $C_{1-exp} = 0.46$. It is absurd to claim agreement between theory and experiment. However, it is interesting to note that the amplitudes of C_{1-th} and C_{1-exp} are fairly close, considering free-slip boundary conditions were used and hence quantitative agreement was not really expected.

3.14 Slow spatial modulation

It is the purpose of this section to show how the effect of spatial modulation may be included into the amplitude equation by using slowly varying spatial coordinates. The source of modulation could be to account for imperfect roll solutions arising from the influence of side-walls. The treatment follows that of Newell and Whitehead 1968. The idea is to include a class of solutions away from criticality, by considering a continuous band of k_n near k_{nc}. We

replace equation (61) by:

$$\vec{w}_0 = \vec{w}_s(X, \tau_4) \begin{pmatrix} 1 \\ \alpha \\ \beta \end{pmatrix} sin\pi z cosk_c x, \tag{109}$$

the amplitude w_0 is a function of the slow time τ and the slow spatial coordinate X. We take $X = \epsilon^2 x$; consequently the second derivative transforms as

$$\frac{\partial^2}{\partial x^2} = \frac{\partial^2}{\partial x_0^2} + 2\epsilon^2 \frac{\partial^2}{\partial x_0 \partial X} + \epsilon^4 \frac{\partial^2}{\partial X^2} = D^2_{c\_x}. \tag{110}$$

We estimate the effect on the amplitude equation (100) by computing the resonant contributions to fifth order. The scaling transforms the linear operator L_0 to

$$L_0 = \begin{pmatrix} \left(\frac{\partial^2}{\partial T^2} + D^2_{c\_x}\right)\left(\frac{\partial^2}{\partial \tau^2} + D^2_{c\_x}\right) w + (1+\psi) D^2_{c\_x}\theta - \psi D^2_{c\_x}\xi \\ \left(\frac{\partial^2}{\partial \tau^2} + D^2_{c\_x}\right)\theta \\ \left(\frac{\partial^2}{\partial \tau^2} + D^2_{c\_x}\right) + L\left(\frac{\partial^2}{\partial \tau^2} + D^2_{c\_x}\right)\xi \end{pmatrix} \tag{111}$$

Secular contributions are derived from terms of the form $\frac{\partial^2 w_0}{\partial X^2}$. The fifth order secular contribution takes the form:

$$\begin{pmatrix} \frac{R_c}{k_c}(1+\psi+\frac{\psi}{L} - 2(\pi^2+3k_c^2) \\ \frac{R_c}{k_c^2} \\ \frac{2R_c}{k^2} \end{pmatrix} \frac{\partial^2 w_0}{\partial X^2} \tag{112}$$

The modified amplitude equation becomes

$$\frac{\partial w_0}{\partial \tau_4} = \alpha w_0 - \beta w_0^3 + \gamma w_0^5 + Q\frac{\partial^2 w_0}{\partial X^2} \tag{113}$$

where

$$Q = (\frac{-R_c}{k_c}(1+\psi\frac{\psi}{L}) + 2(k_c^2 + 3k_c^2) \tag{114}$$

$$+ k^2 + ((1+\psi)\frac{k_c^2}{k^2} - \frac{k^4}{R_c})\frac{2R_c}{k^2}) \tag{115}$$

Equation (111) may be extended to include modulation in the Y direction. The neutral curve would be a curve of radius $\frac{\pi}{\sqrt{2}}$

3.15 Imperfect symmetry

In an experiment, exact symmetry may be thought to hold only approximately. This may be due to the presence of a distant boundary. In a bulk system onset of convection is characterised by a wavelength $\lambda_c = \frac{2\pi}{k_c}$. For a finite box, we may not be able to fit the n paired rolls with the characteristic wave length. In an experiment there are always imperfections, hence Z_2 may be thought to act approximately.

To demonstrate how broken symmetry arises we go back to the mechanical analogue of section (3.2). If we were to tilt the restraining board at a constant angle ϕ we may expect the left-right preference to be broken. We may expect the normal form to be modified by the addition of the lowest order term that breaks the Z_2 symmetry.

We introduce the constant α_0 into the normal form (101) to give:

$$\alpha_0 + w_0(\lambda + \alpha_2 w_0^2 + w_0^4) = 0 \tag{116}$$

with corresponding bifurcation diagram given in fig (7).

3.16 Steinberg approach

An alternative perturbative procedure originally given by Palm et al (1970) was applied to fluids in porous media by Steinberg (1984).

Chapter 4 - the degenerate Hopf bifurcation

4.1 The Hopf bifurcation

The onset of convection in a binary fluid mixture is associated either with a time independent state (a pitchfork or tricritical bifurcation), with a Hopf bifurcation or with a codimension-2 bifurcation associated with both types of instability colliding at a common point in parameter space. In the case of the Hopf bifurcation the flow can consist either of a stationary pattern or more intriguingly, perhaps, of a horizontally translating pattern of rolls (Kolodner 1986). Mathematically this can be found by the imposition of $O(2)$ symmetry on the bifurcation problem. The reflectional symmetry Z_2 corresponds to the left-right symmetry of the roll configuration and the translational symmetry $SO(2)$ refers to the translational invariance of the rolls under a periodic shift. By judicious tuning of experimental conditions both types of patterns have recently been observed in a beautiful series of experiments in $He^3 - He^4$ and ethanol-water systems (Kolodner et al) ,and also in numerical simulations by Knobloch et al 1986.

In this chapter I present a calculation of the pertinent normal form for a pure Hopf travelling wave. Using group theory, Golubitsky and Stewart obtain a generalisation of Hopf's bifurcation theorem given in chapter 2, applicable to ordinary differential equations with symmetry. Golubitsky and Stewart's approach is abstract, by considering the action of $O(n)$ on the Hopf bifurcation. We differ, in that we endeavour to make a firm

connection between the basic equations of motion and the form of the Hopf bifurcation emerging from the presence of $O(2)$ symmetry. Golubitsky and Stewart's perspective is more general in that it treats the general problem of the Hopf bifurcation with symmetry. Their technique, however, cannot be used in a predictive sense; as it cannot tell which bifurcations are physically realised and which are not. The Hopf bifurcation emerging at onset for the separation ratio chosen to be sufficiently negative, may be understood in this more general framework. The translational symmetry $w(x,z,t) \longrightarrow w(x+l,z,t)$, identified with the group $SO(2)$ of rotations of a circle, and reflection; $w(x,z,t) \longrightarrow -w(-x,z,t)$, reflections in the origin or Z_2, are present in the equations governing convection in binary fluid mixtures. The total symmetry of the problem is the direct product of these groups $SO(2) \times Z_2 \cong O(2)$. In addition, a temporal (circle group) symmetry, S^1 arises from the dynamic-phase shift symmetry of the periodic solution of equations (13-15) $w(x,z,t) \longrightarrow w(x,z,t+\theta)$.

Golubitsky and Stewart remark that a doubling of the eigenvalues, $\pm i\omega$ occurs at the Hopf bifurcation point if $O(2)$ symmetry is present. Their remark has direct applicability to the Hopf, travelling wave phenomena in binary fluid mixtures. The aforesaid doubling is merely an observation that the equations admit two wave solutions, each identical, except in their direction of propagation. Therefore, as they are indistinguishable, each wave will bifurcate at precisely the same parameter value.

The usual formulation of Hopf's theorem (see chapter2), without symmetry (except the trivial S^1 symmetry associated with the periodicity of the limit cycle, and the arbitariness of the choice of the origin of time) leads naturally to an equation, concisely written in complex notation, and takes the familiar form:

$$\frac{dA}{dt} = \alpha A + \beta A|A|^2, \qquad A \in C. \tag{117}$$

We can rewrite this in an amplitude-phase represention (polar form); $A = Re^{i\theta}$ where R and θ are functions of time; we obtain:

$$\frac{dA}{dt} = \Re(\alpha)r + \Re(\beta)r^3, \tag{118}$$

$$\frac{d\theta}{dt} = \Im(\alpha) + \Im(\beta)r^2. \tag{119}$$

Treating $\Re(\alpha) > 0$, $\Re(\beta) > 0$, would result in a tricritical Hopf bifurcation in which higher order terms would be important. We shall see later that $\Re(\beta) = 0$ for the Hopf bifurcation in binary fluids i.e. it is degenerate. Golubitsky and Stewart study the classification of the Hopf bifurcation with $O(2)$ symmetry. It turns out that there are other physical situations in which the degenerate Hopf is important, these include the Taylor-Couette experiment (Golubitsky et al 1988) and oscillations in a flexible pipe (Golubitsky et al 1988). Equation(117) is in general supplemented and coupled to an equation describing the counter-propagating wave, of equal amplitude. In general this leads to modulated wavelike behaviour-to be discussed later.

The perturbative procedure used for the degenerate Hopf bifurcation will closely mimic that used in chapter 3, for the standing wave tricritical case.

4.2 Linear theory

Before we discuss linear theory it is important to outline certain approximations we shall make. In the analysis that follows it is essential to choose the non-dimensional quantity A ofequation (1.10), to be zero. This is purely for ease of manipulation of the expansions. This is not a poor approximation considering we can show that convection driven by the Soret and Dufour effects are in fact formally identical problems. By a linear change of coordinates (ξ, θ) we can rewrite the equations in terms of two new variables (ξ', θ'), such that the equations become:

$$\frac{\partial \xi'}{\partial t} + u.\nabla \xi' = \nabla^2 \xi', \tag{120}$$

$$\frac{\partial \theta'}{\partial t} + u.\nabla \theta' = \nabla^2 \theta'. \tag{121}$$

This comment is originally attributable to Knobloch (1980). The variables ξ, θ no longer have a direct physical meaning as did the temperature and the mass flux. Hence, the study of equation (15) with A chosen to be zero is not only a dramatic algebraic simplification, but also the approximation does not detract from the qualitative dynamics expected, even if the contribution due to A turned out to be important. The only problem may arise when we wish to make a quantitative comparison, between experiment and theory.

We consider an oscillatory travelling wave disturbance of the form:

$$w_0 = w_0(\tau)e^{i(\omega t - kx)}\sin(\pi z). \tag{122}$$

By considering waves in both directions a coupled pair of amplitude equations are found by Knobloch (1986), the bifurcation diagram is presented in figure 14, the parameters a and b are given by Knobloch (1986). We substitute (122) into the linearisation, L_t, given by:

$$L_t = \begin{pmatrix} \nabla^2\frac{\partial}{\partial t} - \sigma\nabla^4 & -\sigma\frac{\partial^2}{\partial x^2} & -\sigma\frac{\partial^2}{\partial x^2} \\ -R & \frac{\partial}{\partial t} - \nabla^2 & 0 \\ -\psi R & \psi L\nabla^2 & \frac{\partial}{\partial t} - L\nabla^2 \end{pmatrix}, \tag{123}$$

where we have rexepressed in terms of temperature and concentration variables. For non-triviality of $L_t w_0 = 0$, we obtain an algebraic expression similar to that encountered in chapter 3, for the stationary problem. For wave-like problems this relation is commonly known as a dispersion relation; $det(L_t w_0) = 0$. Two relations will emerge from this consistency condition, one real, one imaginary:

$$\sigma\lambda^2(L\lambda^4 - \omega^2) - \omega^2\lambda^2(1+L) - a^2\sigma R(1 + \psi(1+L)) = 0 \tag{124}$$

for the real part, and

$$-\omega^2 + L\lambda^4(1+L) - \frac{a^2}{\lambda}\sigma R(1+\psi) = 0, \tag{125}$$

for the imaginary part. Together they give an expression for the Rayleigh number as a function of the horisontal wave number, k_x:

$$R = \frac{\lambda^6}{k_x^2\sigma}\frac{\sigma(1-\sigma) - L(1-\sigma)^2L^2(1-\sigma)}{(1-\sigma(1+\psi)} \tag{126}$$

where $\lambda^2 = (\pi^2 - k_x^2)$. By eliminating the Rayleigh number, the linear frequency squared is:

$$\omega^2 = \frac{-\lambda^4}{(1+\sigma(1+\psi)}(\sigma\psi + L\psi(1+\sigma) - L^2(1+\psi)(1+\sigma)). \qquad (127)$$

We make two remarks:

- The R, k dependence of equation (126) is identical to that for the stationary problem. Hence, when a minimum is sought, identically the same critical wave number, $k_{cr} = \frac{\pi}{\sqrt{2}}$ is found.
- For ω to be meaningful ω^2 must be strictly positive, as $\omega^2 < 0$ would give a imaginary frequency; this consequently places a condition on ψ. For small L this means ψ must be negative. This follows from neglecting terms in L^3.

Expressions (124) and (125) may be rewritten as:

$$R_c = R_0\left(1 + \frac{L(1+\sigma)}{\sigma} + \frac{L^2}{\sigma}\right) \qquad (128)$$

and

$$\omega_c^2 = \omega_0^2\left(1 + \frac{L(1+\sigma)}{\sigma} + \frac{L^2(1+\sigma)(1+\psi)}{\psi\sigma}\right), \qquad (129)$$

with

$$R_0 = \frac{\lambda^6(1+\sigma)}{a^2(1+\sigma(1+\psi)}, \qquad (130)$$

and

$$\omega_c^2 = \frac{-\lambda^4\sigma\psi}{(1-\sigma(1-\sigma(1-\psi))}. \qquad (131)$$

These replacements will prove to be useful in the analysis that follows. We expand $\vec{w}$ in a small parameter ϵ, a measure of the small amplitude of the final supercritical state:

$$\vec{w} = \epsilon\vec{w}_0 + \epsilon^2\vec{w}_1 + \ldots, \tag{132}$$

$$\vec{v}_i = \begin{pmatrix} w_0 \\ \theta_0 \\ c_0 \end{pmatrix}, \tag{133}$$

where each term in the series may be thought of as a function of the slow time τ_2. The Rayleigh number is expanded, about R_c, in powers of ϵ.

4.3 $O(\epsilon)$

In general we must take waves in both directions. We choose to take a wave in one direction to simplify the analysis. The form of the equations governing the amplitude of waves propagation in both directions, though more general will reveal the same information about a single wave by simply setting the amplitude of one wave to zero. We equate terms of order ϵ and obtain the following algebraic equation:

$$\begin{pmatrix} -k^2(i\omega + \sigma k^2) & \sigma k_x^2 & \sigma k_z^2 \\ -R_c & i\omega + k^2 & 0 \\ -\psi R_c & -\psi R_c k^2 & i\omega + Lk^2 \end{pmatrix} \begin{pmatrix} 1 \\ \theta_0 \\ c_0 \end{pmatrix} = \vec{0}. \tag{134}$$

Solving for θ_0 and c_0 gives;

$$\vec{w}_0 = w_0 \begin{pmatrix} 1 \\ \frac{R_c}{(i\omega+\lambda)} \\ \frac{\psi R_c}{i\omega+Lk^2}\left(1 + \frac{k^2 L}{(i\omega+k^2)}\right) \end{pmatrix} e^{i(\omega t - kx)} \sin \pi z + \text{c.c.} \tag{135}$$

The complex conjugate ensures that the wave is real. As was the case in chapter 3, an equation for the undetermined multiplier $w_0(\tau)$ must be sought at higher order.

4.4 $O(\epsilon^2)$

At second order we recall the comment made in chapter 3 section, regarding the contribution $w\Delta u - u\Delta w$ being zero in the presence of periodic boundary conditions. This condition still applies. Collating second order contributions we encounter the inhomogeneous equation:

$$Lw_1 = -\pi \begin{pmatrix} 0 \\ \Re(2\theta_0) \\ \Re(2c_0) \end{pmatrix} w_0^2 sin2\pi x, \tag{136}$$

We may readily solve this to give:

$$w_1 = \begin{pmatrix} 0 \\ 1 \\ \frac{\pi(1+\xi_0+\xi^2)(1^2+\pi^2)}{\pi^2+\xi_0 R} \end{pmatrix} |w_0|^2 sin2\pi x \tag{137}$$

The reason for neglecting other contributions is due to how we have expanded the Rayleigh number R. We have chosen R as a series in ϵ^2. The reason for such a choice is exactly as for the stationary bifurcation. To eliminate secularity at second order, recall that $R_1 = 0$ eliminated difficult terms. Armed with the solution to second order we may calculate the relevant contributions to third order from the advective terms $w\nabla\theta + u\nabla\theta$ and $w\nabla c + u\nabla c$.

4.5 $O(\epsilon^3)$

At third order the inhomogeneous equation resembles that obtained at third order in chapter 3. Reserving the details for appendix 5, we obtain:

$$Lw_2 = \frac{R_c k^2}{2(\omega^2 + k^2)} \begin{pmatrix} 0 \\ 1 \\ \frac{\psi(1+L+L^2)k^4+\omega^2}{\omega^2+L^2k^4} \end{pmatrix} |w_0|^2 w_0 (sin3\pi z - sin\pi z) e^{i\chi} + c.c., \tag{138}$$

with $\chi = kx - \omega t$. Recall, potential secularity occurs at third order for the stationary bifurcation analysed in chapter 3; similar behaviour may be seen in equation (138) due to the presence of the term having the same spatial dependence as the solution to first order. Application of the pertinent consistency condition requires the inclusion, at this order of a term proportional to $|w_0|^2 w_0$. If the Rayleigh number, and time, t are scaled by analogy to the calculation presented for the stationary bifurcation, we may obtain a Hopf amplitude equation. It only remains to compute it.

4.6 Calculation of the left eigenvector of L_t

A preliminary step in the ultimate goal of determining a consistency condition for equation (136), and hence in the calculation of the amplitude equation, is in the computation of the left eigenvector, $w_0^\dagger$. Its evaluation is routine and we simply state the result:

$$w_0^\dagger = \begin{pmatrix} 1 \\ \frac{-a^2\sigma(i\omega+(\pi^2+a^2)L(1+\psi)}{(i\omega+L(\pi^2+a^2))(i\omega+(\pi^2+a^2))} \\ \frac{-a^2\sigma}{(i\omega+L(\pi^2+a^2))} \end{pmatrix} \tag{139}$$

4.7 Amplitude equation at third order

The left eigenvector of L_t is used, much in the same way as it was for the stationary problem. We collect together all those terms proportional to $sinwze^{ix}$ from the inhomogeneous contributions and call them. S. We call the rest of the terms S_1, consisting of all other harmonics present. The consistency condition takes the form:

$$< w_0^1(S + S_1) >= 0, \tag{140}$$

where $< . >$ denotes integration over a period in both space variables x and z. This procedure, known as the Fredholm alternative, is actually the main tool of bifurcation theory. The Fredholm alternative can be explained quite simply, either $< w_0^1(S + S_1) >\neq 0$ and $\nexists$ a solution or $< w_0^1(S + S_1) >= 0$ and $\exists$ a solution of dimension = dimension of the kernel. We may simplify this by invoking orthogonality of the basic wavefunctions. We find that we need only those terms in S. The consistency condition reduces to

$$w_0^1 S = 0. \tag{141}$$

We have neglected to integrate over x and z as it merely introduces a trivial constant factor, that multiplies throughout all contributions in S. To eliminate excessive algebra equation(138) will be evaluated in the limit of vanishing Lewis number, L. However, the same conclusion will apply

with non-zero L. For this simpler calculation w_0^1 is take to be:

$$w_0^1 = \begin{pmatrix} 1 \\ \frac{-a^2\sigma}{(i\omega+\lambda^2)} \\ \frac{-a^2\sigma}{i\omega} \end{pmatrix} \tag{142}$$

we obtain

$$p\frac{dw_0}{d\tau} + \left(\tilde{\alpha} + \tilde{\beta}|w_0|^2\right) w_0 = 0 \tag{143}$$

with

$$\begin{aligned} p &= \frac{R_a}{(i\omega+\lambda^2)}\left(\frac{\sigma a^2}{(i\omega+\lambda^2)} + \frac{\sigma a^2 \psi L\lambda^2}{(i\omega+L\lambda^2)(i\omega+\lambda^2)}\right) \\ &+ \frac{\sigma a^2\psi R}{(i\omega+L\lambda^2)(i\omega+L\lambda^2)}\left(1+\frac{L\lambda^2}{(i\omega+\lambda^2)}\right) - \lambda^2 \end{aligned} \tag{144}$$

$$\begin{aligned} \tilde{\alpha} &= \sigma a^2(R-R_a)\left(\frac{1}{(i\omega\lambda^2)} + \frac{\psi}{(i\omega+L\lambda^2)}\right. \\ &+ \left.\frac{\psi L\lambda^2}{(i\omega+L\lambda^2)(i\omega+\lambda^2)}\right) \end{aligned} \tag{145}$$

$$\begin{aligned} \tilde{\beta} &= \frac{-a^2\sigma R_a\lambda^2}{2(\omega^2+\lambda^4)}\frac{\psi(\lambda^4(1+L+L^2)+\omega^2)}{(\omega^2+L^2\lambda^4)(i\omega+L\lambda^2)} \\ &+ \left.\frac{\psi L\lambda^2}{(i\omega+L\lambda^2)(i\omega+\lambda^2)}\right) \end{aligned} \tag{146}$$

$$\begin{aligned} \beta &= \frac{\tilde{\beta}}{p}|_{L=0} \\ &= \frac{-a^2\sigma R_a\lambda^2}{2(\omega^2+\lambda^4)\left(\frac{1}{(i\omega+\lambda^2)} + \frac{\psi(\lambda^2+\omega^2)}{\omega^2}\right)}\frac{R_a}{(i\omega+\lambda^2)}\frac{\sigma a^2}{(i\omega+\lambda^2)} - \frac{\sigma a^2\psi R}{\omega^2} - \lambda^2 \\ &= i\gamma, \end{aligned} \tag{147}$$

$$\gamma = \frac{9\pi(1+\sigma)\omega}{8\sigma w R} \tag{148}$$

The real part of $\mathcal{B}$ vanishes identically (α is not real), hence to obtain a consistent description we seek a method of continuing the expansion to higher order. It is in the expectation that a saturation mechanism can be found to fifth order, that this procedure is performed. Our familiarity with the tricritical bifurcation will guide us as to how to proceed. Let us consider the amplitude $w_0(\tau)$ to be composed of two distinct parts w_{01} and w_{02} such that

$$w_0(\tau) = w_{01}(\tau) + \epsilon^2 w_{02}(\tau), \tag{149}$$

(see Nayfeh and Mook). The scaling and combination is chosen because w_{01} will preserve the amplitude equation to third order. An amplitude equation for $w_{02}(\tau)$ will occur at fifth order. The addition of the two, as prescribed by equation( ) should reveal an equation for $w_0(\tau)$. Alternatively, a second slow time may be introduced, so that w_{02} is also a function of τ_4, see for example Nayfeh and Mook. The result of using both τ_3 and τ_4 instead of the w_{02} leads to exactly the same amplitude equation, with the same coefficients.

4.8 Solution to third order

At third order $w_{02}(\tau)$ does not feature in the consistency condition. The potentially secular terms are, for the moment, neglected. Instead focus on

the contributions due to the advective forcing. This gives:

$$L\vec{w_2^2} = \begin{pmatrix} 0 \\ 1 \\ \frac{\psi(1+L+L^2)\lambda^4+\omega^2}{\omega^2+L^2\lambda^4} \end{pmatrix} |w_0|^2 w_0 sin3\pi z e^{ix} + c.c., \qquad (150)$$

with $\vec{w_2^2} = \frac{R_a\lambda^2}{(\omega^2+L\lambda^4)}$. To solve for $\vec{w_2^2}$ we assume an ansatz of the form $sin3\pi z e^{ix}$ this gives an equation:

$$\begin{pmatrix} -\lambda_1^2(i\omega+\sigma\lambda_1^2) & \sigma a^2 & \sigma a^2 \\ -R_a & i\omega+\lambda_1^2 & 0 \\ -\psi R_a & -\psi R_a\lambda_1^2 & i\omega+L\lambda_1^2 \end{pmatrix} \begin{pmatrix} \vec{w_1} \\ \vec{\theta_1} \\ \vec{c_1} \end{pmatrix} = \begin{pmatrix} 0 \\ 1 \\ \frac{\psi(1+L+L^2)\lambda^4+\omega^2}{\omega^2+L^2\lambda^4} \end{pmatrix}. \qquad (151)$$

All calculations are performed with the Lewis number arbitrary. We may simplify the solutions to each order by considering an experimentally realistic limit. If we choose to express all our results in the limit of vanishing Lewis number, then a dramatic simplification occurs. The solution to the above matrix equation is:

$$\vec{w_2^2} = \frac{3\lambda^2}{\Delta} \begin{pmatrix} a^2\sigma\left(-\left(\frac{1+\sigma}{\sigma}\right)\lambda_1^2 - \frac{i\omega}{\sigma}\right) \\ -\lambda_1^6(1+\sigma) + \lambda_1^2(i\omega+\sigma\lambda_1^2)i\omega \\ -\lambda_1^2(i\omega+\sigma\lambda_1^2)(i\omega+\lambda_1^2\left(\frac{1+\sigma}{\sigma}\right)+\lambda^6(1+\sigma) \end{pmatrix} \qquad (152)$$

with

$$\Delta = (-\omega^2\lambda_1^2(1+\sigma)(\lambda_1^2-\lambda^2)+i\omega(\sigma\lambda_1^6 - Ra^2\sigma(1+\psi)-\omega^2\lambda_1^2). \qquad (153)$$

4.9 $O(\epsilon^4)$

At fourth order we find an equation of the form:

$$L\vec{w_4} = \begin{pmatrix} 0 \\ \mu \\ \varphi \end{pmatrix} |w_0|^4 sin2\pi z, \qquad (154)$$

with,

$$\begin{aligned}
\mu &= -3\lambda^2 3(\lambda^2 + i\omega)a^2\sigma\left[\frac{-\left(\frac{1+\sigma}{\sigma}\right)\lambda_1^2 - \frac{i\omega}{\sigma}}{\Delta}\right] \\
&+ 3(\lambda^2 - i\omega)a^2\sigma\left[\frac{-\left(\frac{1+\sigma}{\sigma}\right)\lambda_1^2 - \frac{i\omega}{\sigma}}{\Delta}\right] \\
&+ \frac{2(-\lambda^6(1+\sigma) + \lambda_1^2(i\omega + \sigma\lambda_1^2)i\omega}{\Delta} \\
&+ \frac{2(-\lambda^6(1+\sigma) + \lambda_1^2(-i\omega + \sigma\lambda_1^2) - i\omega}{\Delta}
\end{aligned} \tag{155}$$

$$\begin{aligned}
\varphi &= -3i\omega\left(\frac{1+\sigma}{\sigma}\right)\left[\frac{-\left(\frac{1+\sigma}{\sigma}\right)\lambda_1^2 - \frac{i\omega}{\sigma}}{\Delta}\right] \\
&+ 3i\omega\left(\frac{1+\sigma}{\sigma}\right)\left[\frac{-\left(\frac{1+\sigma}{\sigma}\right)\lambda_1^2 - \frac{i\omega}{\sigma}}{\Delta}\right] \\
&+ \frac{2(-\lambda^6(1+\sigma) + \lambda_1^2(i\omega + \sigma\lambda_1^2)i\omega}{\Delta} \\
&+ \frac{2(-\lambda^6(1+\sigma) + \lambda_1^2(-i\omega + \sigma\lambda_1^2) - i\omega}{\Delta}
\end{aligned} \tag{156}$$

At this stage we begin to realise the need for a simplification therefore the Lewis number is chosen to be zero. The expressions become considerably more tiresome to manipulate. We first solve at fourth order by retaining the notation of third order. This is preferable to expressing everything in terms of the original variables. Again, we absorb a multiplicative factor into a new scaled variable, $\tilde{w}_0$.

$$w_4 = -\frac{3\lambda^3|w_0|^4\pi\tilde{w}_4}{|\Delta|^2} \tag{157}$$

We solve for an assumed ansatz of the form:

$$\hat{\theta}_4 = \frac{\mu}{4\pi^2} \tag{158}$$

$$\hat{c}_4 = \frac{\varphi + \psi L\mu}{4\pi^2 L} \tag{159}$$

Also, at this order one picks up terms of the form $w_1^* w_0$. All of these contribute to the cubic portion of the consistency condition. However, as this and the third order amplitude equation for w_0 are added we reestablish the third order anomaly.

The amplitude equation to fifth order takes the form:

$$\frac{dw_1}{d\tau_4} = \alpha w_1 - \beta(w_0 w_1^* + \bar{w}_0^* w_1) w_0 - \beta|w_0|^2 w_1 \tag{160}$$

$$- \gamma|w_0|^4 w_1, \tag{161}$$

with,

$$\gamma = \frac{-\sigma\pi^3}{3\omega^2|\Delta|^2} M \tag{162}$$

and

$$M = \left(\left(\frac{1+\sigma}{\sigma}\right)\hat{\theta}_4 + \hat{c}_4\right)\left(\frac{9\pi^4\sigma\omega^2}{R_c} - i\omega\pi^2\left(1 + \frac{27\pi^4\sigma}{R_c}\right)\right) \tag{163}$$

and we note that the real part of γ is positive; this can be confirmed numerically. Recall, the total amplitude is $w_0 = w_{01} + \epsilon^2 w_{02}$, then to order ϵ^3, by adding equations (160) and (143), we obtain:

$$\frac{dw_0}{d\tau} = \alpha w_0 - \beta|w_0|^2 w_0$$

$$- \epsilon^2\gamma|w_0|^4 w_0. \tag{164}$$

We can conclude from the above expression that, unlike the tricritical bifurcation which was hysteretic, we obtain a purely degenerate forward Hopf bifurcation. Also, if we consider γ to be an expansion in L, then the coefficient γ has a dominant term that is independent of L, in a non-trivial sense. The dependence of γ on the other physical parameters, such as the Prandtl number, may be of interest but is most efficiently investigated numerically.

4.10 Predictions versus reality

Recent experiments performed in the vicinity of R_{st} for binary fluid mixtures confirm the thesis that for large aspect ratio cells the travelling wave state is stable. This claim is also substantiated in a faithful two-dimensional simulation of the full two-dimensional partial differential equations. This calculation was performed in a large aspect ratio cell by Moore and coworkers. However, there still remain a number of discrepancies with the present theory. Apparently, the most damning is the prediction of a forward Hopf bifurcation; this is not seen in experiment. What is observed is a hysteretic Hopf. Rather than abandonning the theory, is it possible to understand this phenomenon within the context of the present analysis? The answer is yes and certainly within the context of equivariant bifurcation theory - such behaviour may be seen in the unfolding of the bifurcation . To perform the calculation properly would require recourse to the 'real' boundary conditions. The reason that $\Re(\beta)$ vanishes identically is not entirely obvious and seems to be a residue of the simple periodic boundary conditions chosen. By

projecting onto a more realistic set of equations by the method of Galerkin reveals that $\Re(\beta)$ does not vanish; this observation will be discussed more completely in chapter 5.

The experiments demonstrate that the travelling wave branches subcritically, inferring that $Re(\beta) > 0$. Although in $He^3 - He^4$ bulk mixtures we fail to be able to observe the flow directly, one can infer bifurcation behaviour indirectly by measurement of the non-dimensional heat transport, or Nusselt number. For a travelling wave the Nusselt number is a constant, since the oscillation is averaged over the whole cell. For the stationary Hopf bifurcation we should expect that the Nusselt number will fluctuate with the underlying oscillatory frequency.

In ethanol-water and $He^3 - He^4$ mixtures Kolodner et al observe a hysteric branched Hopf state, and this is confirmed by the appropriate Nusselt plot. However, we may observe the stationary Hopf bifurcation in more restricted geometries. In $He^3 - He^4$ mixtures in a porous medium[1](see Dullien 1975 and Brand 1984 and references therein), this bifurcation has been reported.

Considering the aspect ratio has such an important role in determining

[1]The equations describing convection in a porous medium are based on Darcys law (ref. 13). Also, the advective nonlinearity in the equation for the velocity field $\vec{v}\nabla\vec{v}$ is replaced by a term proportional to $\vec{v}|\vec{v}|$. The coefficient that multiplies this term is physically very small; as a result the equation for the velocity field is linear. In the presence of periodic boundary conditions the results, therefore, for the bulk binary fluid and a binary fluid in a porous medium are almost the same in that the nonlinearity in the equation for the velocity field is taken to be identically zero. This will be the source of degeneracy in the calculated normal forms.

dynamical behaviour then perhaps we should be thinking in terms of a codimension-3 description. The form of this codimension-3 description is unclear, because the effect of finite lateral walls is not known in an analytical form. Perhaps the best attempt to circumvent this impasse is given by Cross, in which he considers the reflection of a travelling wave off the lateral boundaries. A reflection with reflection coefficient 1 (completely reflected) corresponds to a standing wave. In experiments performed by a group at AT&T Bell laboratories, Kolodner and coworkers see such behaviour. In the centre of their cell they observe a standing wave pattern constructed from left and right travelling waves.

Current research is concentrated on the codimension-2 bifurcation. This bifurcation structure results from the collision in parameter space of the stationary and Hopf bifurcations. When this is based on idealised boundary conditions, several discrepancies arise. It is becoming clear that experiments may be understood in a more general framework. For example, allowing imperfect boundaries into the theory introduce phenomenological unfolding parameters that break the overall exact symmetry. Also, the use of envelope equations of the Newell-Whitehead-Segal type may be useful as they affect the dynamics. However, the effect of spatial modulation is unclear, even in its effect on linear stability.

4.11 Equivariant bifurcation theory for the degenerate and non-degenerate Hopf bifurcation

It is instructive to discuss the Hopf bifurcation in the presence of symmetry, in the context of equivariant bifurcation theory. It will serve to provide a framework in which both the degenerate and nondegenerate Hopf bifurcation may be discussed. As the critical eigenspace is doubled in the presence of $O(2)$ symmetry the problem is four-dimensional. We consider complex amplitudes A and B and write our basic travelling wave ansatz as:

$$w_0 = [(A+B)e^{i\omega_0 t} + (A^* + B^*)e^{i\omega_0 t}]\sin\pi x \tag{165}$$

where A and B are functions of time. The first step in the analysis is in the construction of invariants under the $O(2)$ action. We note that there are three:

$$i_1 = |A|^2 + |B|^2 \tag{166}$$

$$i_2 = AB^* \tag{167}$$

$$i_3 = BA^* \tag{168}$$

If we construct our vector field from these invariants then the subsequent flow will be invariant under the symmetry. The most general form this can take to third order in A and B assuming certain non-degeneracy conditions is

$$\begin{pmatrix} \dot{A} \\ \dot{B} \end{pmatrix} = \begin{pmatrix} i\omega_0 A & 0 \\ 0 & -i\omega_0 B \end{pmatrix} \tag{169}$$

$$- \begin{pmatrix} f_1 A - f_2 B \\ f_2^* A + f_1^* B \end{pmatrix} \tag{170}$$

with f_1 and f_2 chosen to be

$$f_1 = \alpha_1(|A|^2 + |B|^2) + \beta_1 AB^* + \gamma_1 BA^* \tag{171}$$

$$f_1 = \alpha_2(|A|^2 + |B|^2) + \beta_2 AB^* + \gamma_2 BA^* \tag{172}$$

By introducing a near identity nonlinear coordinate change given by;

$$A = \hat{A} + \alpha|A|^2 A + \beta|B|^2 A + \gamma|A|^2 B^* \tag{173}$$

$$+ \delta|A|^2 B + \epsilon|B|^2 B + \eta B^2 A^*, \tag{174}$$

$$B = \hat{A} + \alpha^*|B|^2 B + \beta^*|A|^2 B + \gamma^*|B|^2 A^* \tag{175}$$

$$+ \delta^*|B|^2 A + \epsilon^*|A|^2 A + \eta^* A^2 B^*, \tag{176}$$

we express in terms of $\hat{A}$ and $\hat{B}$ utilising the following results to 0(3):

$$(|B|^2 A) = i\omega_0|\hat{B}|^2\hat{A} \tag{177}$$

$$(A^2 B^*) = 3i\omega_0 \hat{A}^2\hat{B}^* \tag{178}$$

$$(|A|^2 B) = -i\omega_0|\hat{A}|^2\hat{B} \tag{179}$$

$$(|B|^2 B) = -i\omega_0|\hat{B}|^2\hat{B} \tag{180}$$

$$(B^2 A^*) = -3i\omega_0 \hat{B}^2\hat{A}^* \tag{181}$$

$$(|A|^2 A) = i\omega_0|\hat{A}|^2\hat{A}. \tag{182}$$

where the dot denotes differentiation with respect to t. The purpose of such a transformation is to reduce the equation to its simplest form without changing the topology of the bifurcation. This gives:

$$\dot{\hat{A}} = i\omega_0\hat{A} + \hat{A}^2\bar{B}^*(-2\gamma i\omega_0 + C) + |\hat{A}|^2\hat{B}(2\delta i\omega_0 - D) \quad (183)$$

$$+ |\hat{B}|^2\hat{B}^*(2\varepsilon i\omega_0 + E) + |\hat{B}|^2\hat{A}^*(4\eta i\omega_0 + F) \quad (184)$$

$$+ P|\hat{A}|^2\hat{A} + Q|\hat{B}|^2\hat{A}. \quad (185)$$

Hence, by choosing the following values for the constants;

$$\gamma = \frac{C}{2i\omega_0}, \delta = \frac{-D}{2i\omega_0}, \quad (186)$$

$$\varepsilon = \frac{-E}{2i\omega_0}, \eta = \frac{-F}{4\eta i\omega_0} \quad (187)$$

we may eliminate the first four cubic terms using this procedure. Similarly, for an equation for $\dot{w}$ we finally obtain to third order two equations:

$$\dot{\hat{A}} = i\omega_0\hat{A} + P|\hat{A}|^2\hat{A} + Q|\hat{B}|^2\hat{A} \quad (188)$$

$$(\dot{\hat{B}}) = i\omega_0\bar{B} + P|\hat{A}|^2\bar{B} + Q|\bar{B}|^2\bar{B}. \quad (189)$$

These are canonical equations for the Hopf bifurcation with $O(2)$ symmetry. In nongeneric circumstances in which $\Re(Q) = 0$ we find the amplitude equations are of an adequate order. The corresponding bifurcation diagram is shown in fig (14).

If we expand equation (170) to higher order, anticipating a degeneracy in the coefficients we obtain:

$$\dot{A} = A_1 + (b_1|B|^2 + c_1(|A|^2 - |B|^2) + d_1|B|^4 \quad (190)$$

$$+ \quad f_1|B|^2(|A|^2+|B|^2)A + g_1|B|^6A + h_1(|A|^2+|B|^2)^3A \qquad (191)$$

$$+ \quad i_1(|B|^2(|A|^2+|B|^2)^2)A + k_1(|B|^4(|A|^2+|B|^2))A \qquad (192)$$

with the change of variables given by:

$$\hat{A} = A + \alpha(|A|^2+|B|^2)^2A + \beta(|A|^2+|B|^2)B^2A + \gamma B^4A. \qquad (193)$$

$$\hat{B} = B + \alpha(|A|^2+|B|^2)^2B + \beta(|A|^2+|B|^2)A^2A + \gamma A^4B, \qquad (194)$$

to give dropping the hats;

$$\dot{A} = c_1(|A|^2+|B|^2)A + e_1(|A|^2+|B|^2)^2A \qquad (195)$$

$$= f_1|B|^2(|A|^2+|B|^2)A + d_1|B|^4A + g_1|B|^6A \qquad (196)$$

similarly,

$$\dot{B} = c_1(|A|^2+|B|^2)B + e_1(|A|^2+|B|^2)^2B \qquad (197)$$

$$= f_1|B|^2(|A|^2+|B|^2)B + d_1|B|^4B + g_1|B|^6B. \qquad (198)$$

We are interested in the primary branched state and hence a fifth order truncation suffices, for higher order branched states (secondary and even tertiary) the description of the amplitude equations must be to seventh order; see remark made by Knobloch (1986).

4.12 $\Re(\beta) = 0$

It is particularly intriguing why the two-component convection problem has a degeneracy such that $\Re(\beta) = 0$. All attempts to explain this are

based upon calculation (E. Knobloch (1986), J. Swift (1984) and references therein). It would seem that a more elegant explanation should exist: perhaps in terms of a hidden symmetry argument (Dangelmayr and Armbruster (1986)). However, it is uncertain that this is the way to proceed. It is clear that this is an avenue for future research.

Chapter 5 - Schemes of Galerkin truncations

5.1 The method of Galerkin

The origin of the method of Galerkin is generally associated with a paper published by Galerkin (1915) on the elasic equilibrium of rods and thin plates.

The Galerkin technique has been applied to many problems. A major difficulty turns out to arise from how to handle the convection-dissipation interaction correctly. The key feature of the Galerkin method may be stated quite concisely. We will assume a two-dimensional problem is governed by a linear differential equation (we shall see that this may be extended to include a class of nonlinear problems). Consider:

$$L(w) = 0 \tag{199}$$

in the domain $D(x, y)$, with boundary conditions

$$S(w) = 0 \tag{200}$$

on $\partial D(x, y)$, the boundary of $D(x, y)$. The Galerkin method assumes that w can be accurately represented by an approximating solution, w_a.

$$w_a = w_0(x, y) + \sum_{j=1}^{N} a_j \phi_j(x, y), \tag{201}$$

where the ϕ_j's are known analytical functions (moreover in the cases we consider ϕ_j's are separable), w_0 is introduced to satisfy the boundary conditions and a_j are the coefficients to be determined. Substitution of equation

(201) into (199) produces a non-zero residual, R, given by

$$R = L(w_a) = L(w_0) + \sum_{j=1}^{N} a_j L(\phi_j) \tag{202}$$

In the Galerkin method the unknown coefficients, a_j in equation (201) are obtained by solving the following system of equations:

$$< R, \phi_k >= 0 \qquad k = 1, ..., N. \tag{203}$$

Here R is the relevant equations residual, the ϕ_j's are the same functions that appear in the expansion and $<,>$ is an inner product. Since this example is based on a linear differential equation, (203) can be written as a matrix equation for the coefficients a_j as

$$\sum_{j=1}^{N} a_j < L(\phi_j), \phi_k >= - < L(w), \phi_k > . \tag{204}$$

Substitution of a_j's resulting from the solution of (204) gives the required approximate solution w_a. It is convenient to define the inner product $< f, g >$ in the following manner:

$$< f, g >= \int \int_D fg dx dz. \tag{205}$$

The method of Galerkin has been used to simplify the study of certain partial differential equations, and to represent them by an approximate, simpler set of equations. This simpler set, takes the form of a finite number of ordinary differential equations. The technique is well suited to fluid flow problems as the expansion is known to converge strongly to the exact

solution in the case of the two-dimensional Navier-Stokes equation. In the three-dimensional case a number of weaker results are known (Ladyzhenskaya 1963 and 1978). Performing an expansion in a complete set leads to an infinite set of ordinary differential equations. Clearly, this is unsatisfactory as a infinite dimensional system is as difficult as the original equations to determine dynamical behaviour for. We must accordingly truncate, to include only a finite number of modes.

The number of modes, which I will take to mean approximating functions, required to capture the true nonlinear character of the equations is difficult, in general, to estimate. The approach by Temam and Foias based on functional analysis estimates has shown that there is a theoretical basis for determining the qualitative long term behaviour of a fluid and this can be achieved by the study of a finite but sufficient number of modes.

The success of the method of Galerkin relies on providing a good trial ansatz, for the dependent quantities of the velocity, temperature and concentration. This usually takes the form of an expansion in a set of functions (for example polynomials, spherical harmonics or a fourier series), with arbitrary, time dependent coefficients. The error inherited by the assumption of a finite, non-exact solution, is minimised by averaging over the flow. This averaging takes the form of integrating over the spatial coordinates in the fluid domain. In the two dimensional case this is in x and z. The problem of solving, or determining the dynamics, even numerically is reduced dra-

matically. In general, we are now faced with studying a set of non-linear ordinary differential equations. If the truncation is taken to a high order (in excess of one hundred modes, say), then task of investigating the equations does start to become numerically cumbersome, although much larger systems have been investigated (Yahata 1984).

The O.D.E's arising from such truncation are easily investigated using a number of existing numerical packages. The most commonly available that serves to produce adaquate and accurate results is by the Nottingham Algorithms Group (NAG). The NAG routines used are based upon high order Runge-Kutta methods. More sophisticated packages exist such as AUTO, to investigate bifurcation behaviour, and are widely avaliable. The aim of chapter 5, therefore, is to study some aspects of Galerkin schemes applied to convection in binary fluid mixtures. The initial objective will be to obtain a sufficiently reduced model to describe behaviour near bifurcation points exactly. It will not be in the spirit of Temam and Foias, in the sense that we do not wish to obtain strong convergence results over a large parameter range, as that will be at the expense of high dimensionality. We will seek to obtain a low dimensional scheme that retains the essential dynamics observed in the actual flow, close to criticality. A Veronis 'minimal representation' (Veronis 1963) will begin as our first guess and we shall build upon this minimal system. The reason for studying such truncation schemes, over and above the bifurcation behaviour it mimics at criticality,

is that they may be useful for the investigation of larger amplitude phenomena, conjecturing that the low dimensional approximation is still valid. In this way we may possibly elucidate typical or generic behaviour.

5.2 Truncation schemes for binary fluid mixtures

We present the derivation and numerical results for a set of Galerkin truncation schemes for convection in binary fluids. We expect to be able to describe the dynamical behaviour for Rayleigh numbers chosen close to criticality by a set of truncated model equations. Five and eight mode truncation schemes are derived assuming a stationary solution with time dependent coefficients. The five mode model is formally equivalent to that model studied by Knobloch et al for the thermohaline problem. The two systems differ only by a linear change of dependent variables. The dynamical behaviour for the two truncations will be identical. However, the question remains, how do the dynamics change as the order of the truncation is increased? We will try to cast some light on this question.

5.2.1 How do we truncate?

There are no general practical rules of truncation to a finite system of equations which adequately describes the dynamics of the original equations. The sufficient number of modes required for a faithful representation of a flow is in general very, very large. However, the dimension[2] of the

[2] dimension = dimension of the natural measure

attractor for a fluid flow has been determined experimentally: in suitably constructed phase space for the Taylor-Couette experiment it is found to be small (Gollub 1985). Foias et al discuss the sufficient number of vector valued functions to maintain a good estimate of the underlying flow. For the single fluid problem and for Grashof numbers, $Gr = \frac{R}{\nu} \approx 5 \times 10^4$, Foias et al report that 10^5 modes are required for two-dimensional flow and as many as 10^{16} modes for the full three dimensional flow. Moreover, they observe that the addition of more modes is not a good rule to necessarily improve the accuracy of the approximation. Their estimates are based on a functional analysis approach.

An estimate of the dimension of the 'attractor' in an experimental Taylor-Couette system puts its value in the chaotic regime at approximately five. We must treat this result with some sceptism as there is great uncertainty in the the measurement of the dimension of the attractor, as we must remember the spatial dynamics have been largely ignored. However, irrespective of the actual numerical value the very fact that its value is measured to be small indicates that the number of degrees of freedom needed to describe the dynamics in this regime is perhaps small. If the measured dimension turns out to be large then a low dimensional description would be futile. One must also realise that the figures quoted from Temam's work are upper bounds, and I expect poor ones at that, so the situation may not be as gloomy as the functional analysis approach suggests.

5.3 The truncation heirarchy

In order to fulfil the Foias criterion I have suggested that we need an inordinate number of modes to accurately represent the flow. In our model system we retain only a few modes, taking full advantage of the spatially periodic structure of the flow even up to the onset of temporal chaos (ref Libchaber).

In this respect, the low dimensional approximation is flawed as we heavily rely on experimental input for guidance. The alternative approach is to pursue a high dimensional system. This is computationally expensive and further more becomes analytically intractable. The hope is that the flow at modest Rayleigh numbers is describeable by a low dimensional system of equations.

The low dimensional Lorenz-like truncation schemes, constructed with a stationary ansatz, is thought to be relevant in small aspect ratio experimental cells. The smallness of the aspect ratio ensures only a small number of modes can possibly be excited. (An analogous effect is observed in a short stretched string in which the length of the string determines the number of modes one can excite).

Conversely, a travelling wave associated with the Hopf bifurcation is relevant to a large aspect ratio system - in effect infinite. A Galerkin truncation scheme based on a travelling wave ansatz is no longer applicable to a small aspect ratio cell. However, we would expect a large aspect

ratio cell to allow many more competing modes. Near bifurcation points this competition is well characterised: however away from these special points the interaction of modes may be extremely intricate. It is with this proviso that we need to treat the travelling wave truncation scheme of low order with some sceptism, especially when probing regions of large Rayleigh number (typically, $R > 2 - 3 \times R_c$).

We choose to investigate rectangular cells; cylindrical cells may be treated in an analogous fashion. Hence, the truncation scheme reduces to truncating a double fourier series.

5.4 Galerkin truncation of Lorenz and Saltzmann

Perhaps the first recognisable account of a Galerkin truncation scheme being used as a tool for investigation of a hydrodynamical instability was by Saltzmann in 1962. In the following year a remarkable paper by Lorenz, based on Saltzmann's work and comprising a numerical study of a severely truncated scheme, for the single fluid Benard problem, was published.

Lorenz 1963 had discovered that in his system of three ordinary differential equations irregular fluctuations, or as he originally phrased it-aperiodicity occurred. The importance of the paper was to prove to be profound. His discovery was incredibly important to physical scientists, in that the model was derivable from a physically realisable situation (albeit using a severely truncated scheme) and hence eradicated the ingrained belief that regularity and periodicity was all one could expect from such simple

equations. It was also an important contribution in that it would help to elucidate one of the longest standing probems in physics: the problem of turbulence. Twenty-five years on from the appearance of Lorenz's paper we are perhaps no closer to understanding the problem of strong turbulence. However, low dimensional turbulence has been experimentally verified and it seems to fit the overall picture of low dimensional chaos.

Features of 'aperiodicity' can be seen in similar truncation schemes (Franchescini). Also, many physical systems have been modelled with some confirmable success. The pumped laser has been modelled by truncation of the Maxwell-Bloch equations by Haken. The Maxwell-Bloch equations are the continuum equations that govern the electronic excitation in atoms. Irregular behaviour has been observed experimentally.

Chapter 5 will contain a study of a sequence of Lorenz like truncations for the binary fluid equations. Although the Galerkin truncation scheme is not unique, the choice of modes will be motivated by the choice of ansatz in chapters 3 and 4. It has been known since Lorenz's seminal work in 1963 that complicated behaviour can result from very simple severely truncated schemes. The five mode model we shall derive and discuss arose from a Veronis 'minimal representation'. We include only those modes that go to describe the instability at onset (for the stationary bifurcation). In the limit of vanishing concentration gradient the equations decouple and reduce to those of Lorenz. We may include the tricritical bifurcation in the

zoology of dynamical behaviour in a truncated model by extending from five to eight modes. The tricritical bifurcation demands the inclusion of the modes proportional to $\overline{w}sin3\pi zcosk_x x$. These three modes (for the velocity, temperature and concentration) are included in addition to the usual Veronis model. An eight and a fourteen mode model can be constructed in an analogous fashion, the choice being dictated by the assumptions made in chapter 4. A brief numerical investigation is given.

5.5 Aside: an alternative approach

Before describing the truncation schemes, let us first analyse an alternative approach. An alternative to the use of an arbitrary trunction, albiet legitimate near the bifurcation point, which results in a low dimensional set of O.D.E's instead of utilising the eigenfunctions of the minimal representation is to use a so called proper orthogonal projection (p.o.p). This technique, initiated by Lumley tries to select out unbiasedly only those modes which are important. The importance of a normal mode is determined by calculating its auto-correlation function. From it we can decide how well correlated a given arbitrarily chosen mode is to the experimental data. Aubrey et al hasled recent effort to use this technique, to elucidate coherent structures in the wall region of a turbulent boundary layer. When would we use such a technique? It would seem appropriate to use p.o.p. most usefully in parameter regimes away from points of bifurcation. as it is usually clear what to use in these regions. In a turbulent regime. for

instance. where it is suspected that the dynamics are governed by a low number of modes, the technique may be most powerful. The power of the approach is that it is semi-empirical and hence does not rely on arbitrary choice of modes. This approach seems to have much promise and perhaps should be the subject of extensive future investigation.

5.6 The stationary bifurcation

5.6.1 Five mode model

The five mode truncation using Veronis' "minimal representation" has been considered by Knoboch et al. The choice of the 5 modes that compose the minimal representation is chosen so as to reproduce to second order, the perturbative approach for the stationary bifurcation.

In a similar fashion it is natural to extend these ideas to higher order truncations. A general expansion will be of the form:

$$w = \sum_{m=1}^{M} \sum_{n=1}^{N} W_{mn}(t) cos(mk_x x) sin(n\pi z) \tag{206}$$

$$\theta = \sum_{m=1}^{M} \sum_{n=1}^{N} \theta_{mn}(t) cos(mk_x x) sin(n\pi z) \tag{207}$$

$$c = \sum_{m=1}^{M} \sum_{n=1}^{N} c_{mn}(t) cos(mk_x x) sin(n\pi z). \tag{208}$$

Expansions of this form automatically satisfy the periodic boundary conditions imposed. The expanded functions w, θ and c are defined over the domain (0,1) in z and over all x. Also, we do not necessarily have to choose all modes up to and including M and N.

5.6.2 5-mode Veronis minimal representation

We consider a subset of the expansion given above, choosing the modes:

$$w = X_1(t) sin\pi z cosk_x x \tag{209}$$

$$\theta = Y_1(t)sin\pi zcosk_c x + Z(t)sin2\pi z \tag{210}$$

$$c = U_1(t)sin\pi zcosk_c x + V(t)sin2\pi z \tag{211}$$

These expansions are substituted into the basic equations of motion (13-15). Five equations are obtained by multiplying by the relevant mode and integrating. The equation for X_1 is derived from the equation for the velocity, Y_1, Z result from the equation for the temperature. The equation for the concentration gives equations for U_1 and V. The integration is performed on x from 0 to $\frac{\pi}{k_c}$ and on z from 0 to 1. The orthogonality conditions of the trigonometrical functions are used. In this way the time evolution of each fourier component is obtained.

$$\dot{X}_1 = -\sigma(X_1 - Y_1 - U_1) \tag{212}$$

$$\dot{Z} = -\frac{8}{3}Z + X_1 Y_1 \tag{213}$$

$$\dot{Y}_1 = -Y_1 - rX_1 - ZX_1 \tag{214}$$

$$\dot{V} = -\frac{8}{3}L(V - \psi Z) + X_1 U_1 \tag{215}$$

$$\dot{U}_1 = -L(U_1 - \psi Y_1) + RX_1 = -VX_1 \tag{216}$$

The form of the expansion means that the integrations are trivial, in as much, we may determine the equation for X_1 by comparing like modes. For example, to determine the equation for X_1 we compare all those terms proportional to $sin\pi cosk_c x$. The equations for the other modes follow similarly.

5.6.3 8-mode representation

An extended version of the minimal representation includes three further modes. X_3, Y_3, U_3:

$$w = X_1(t)sin\pi zcosk_c x + X_2(t)sin3\pi zcosk_c x \quad (217)$$

$$\theta = Y_1(t)sin\pi zcosk_c x + Y_2(t)sin3\pi zcosk_c x + Z(t)sin2\pi z \quad (218)$$

$$c = U_1(t)sin\pi zcosk_c x + U_2(t)sin3\pi zcosk_c x + V(t)sin2\pi z \quad (219)$$

The process outlined for the 5-mode model is repeated and a set of eight nonlinear O.D.E's result:

$$-\lambda_1^2(\dot{X}_1 + \sigma\lambda_1^2 X_1) = -k_c^2\sigma(Y_1 + U_1) \quad (220)$$

$$-\lambda_3^2(\dot{X}_2 + \sigma\lambda_3^2 X_2) = -k_c^2\sigma(Y_2 + U_2) \quad (221)$$

$$\dot{Z} + (2\pi)^2 Z = \frac{\pi}{2}(-X_1Y_1 + X_2Y_1 + X_1Y_2) \quad (222)$$

$$\dot{Y}_1 + \lambda_1^2 Y_1 - RX_1 = \pi Z(X_1 - X_2) \quad (223)$$

$$\dot{Y}_2 + \lambda_2^2 Y_1 - RX_2 = -\pi Z X_2 \quad (224)$$

$$\dot{V} + 4\pi^2 L(V - \psi Z) = \frac{\pi}{2}(-X_1U_1 + X_2U_1 + X_1U_2) \quad (225)$$

$$\dot{U}_1 + L\lambda_1^2(U_1 - \psi Y_1) - \pi RX_1 = \pi V(X_1 - X_2) \quad (226)$$

$$\dot{U}_2 + L\lambda_3^2(U_2 - \psi Y_2) - \pi RX_2 = -\pi X_2, \quad (227)$$

where $\lambda_1^2 = (\pi^2 + k_c^2)$ and $\lambda_1^2 = ((3\pi)^2 + k_c^2)$. We rescale the variables using:

$$\frac{\lambda_1^2}{k_c} X_1 \longrightarrow X_1 \quad (228)$$

$$\frac{\lambda_1^2}{k_x^2} X_1 \longrightarrow X_1 \tag{229}$$

$$\frac{\lambda_1^2}{k_x^2} Y_1 \longrightarrow Y_1 \tag{230}$$

$$\frac{\lambda_1^2}{k_x^2} Y_2 \longrightarrow Y_2 \tag{231}$$

$$\frac{\lambda_1^2 2\pi Z}{\pi^4} \longrightarrow Z \tag{232}$$

$$\frac{\lambda_1^2 2\pi V}{\pi^4} \longrightarrow V \tag{233}$$

$$\frac{\lambda_1^2}{k_x^2} U_1 \longrightarrow U_1 \tag{234}$$

$$\frac{-\lambda_1^2}{k_x^2} U_2 \longrightarrow U_2, \tag{235}$$

scaling time as:

$$\frac{d}{dt} \longrightarrow \lambda_1^2 \frac{d}{dt}. \tag{236}$$

These substitutions serve to eliminate extraneous constants. The eight-mode model becomes:

$$\dot{X}_1 = -\sigma(X_1 - Y_1 - U_1) \tag{237}$$

$$\dot{X}_2 = -\sigma(\frac{19}{3} X_2 - \frac{3}{19} Y_2 - \frac{3}{19} U_2) \tag{238}$$

$$\dot{Z} = -\frac{8}{3} Z + (X_1 Y_1 + X_2 Y_1 + X_1 Y_2) \tag{239}$$

$$\dot{Y}_1 = -Y_1 - r X_1 - Z(X_1 + X_2) \tag{240}$$

$$\dot{Y}_2 = \frac{19}{3} Y_2 - r X_2 - Z X_2 \tag{241}$$

$$\dot{V} = -\frac{8}{3} L(V - \psi Z) - (X_1 U_1 + X_2 U_1 + X_1 U_2) \tag{242}$$

$$\dot{U}_1 = -L(U_1 - \psi Y_1) + \psi R X_1 + -V(X_1 + X_2) \tag{243}$$

$$\dot{U}_2 = -L(\frac{19}{3}U_2 + \frac{19}{3}\psi Y_2) - wRX_2 - X_2V. \quad (244)$$

5.6.4 14-mode representation

Extending the model still further by including the modes conjugate to X_1, X_2, Y_1, Y_2, U_1, U_2 and so allowing travelling wave states, we obtain a 14-mode representation:

$$w = X_1(t)sin\pi zcosk_c x + X_2(t)sin3\pi zcosk_c x \quad (245)$$

$$+ \bar{X}_1(t)sin\pi zsink_c x + \bar{X}_2(t)sin3\pi zsink_c x \quad (246)$$

$$\theta = Y_1(t)sin\pi zcosk_c x + Y_2(t)sin3\pi zcosk_c x + Z(t)sin2\pi z \quad (247)$$

$$+ \bar{Y}_1(t)sin\pi zsink_c x + \bar{Y}_2(t)sin3\pi zcosk_c x \quad (248)$$

$$c = U_1(t)sin\pi zsink_c x + U_2(t)sin3\pi zcosk_c x + V(t)sin2\pi z \quad (249)$$

$$+ \bar{U}_1(t)sin\pi zsink_c x + \bar{U}_2(t)sin3\pi zsink_c x \quad (250)$$

We scale as we have scaled using relations (18-26), where the conjugate quantities are scaled in the same way.. This gives:

$$\dot{\bar{X}}_1 = -\sigma(\bar{X}_1 - \bar{Y}_1 - \bar{U}_1) \quad (251)$$

$$\dot{\bar{X}}_1 = -\sigma(\bar{X}_1 - \bar{Y}_1 - \bar{U}_1) \quad (252)$$

$$\dot{X}_2 = -\sigma(\frac{19}{3}X_2 - \frac{3}{19}Y_2 - \frac{3}{19}U_2) \quad (253)$$

$$\dot{\bar{X}}_2 = -\sigma(\frac{19}{3}\bar{X}_2 - \frac{3}{19}\bar{Y}_2 - \frac{3}{19}\bar{U}_2) \quad (254)$$

$$\dot{Z} = -\frac{8}{3}Z + X_1.Y_1 + X_2.Y_1 + X_1.Y_2) \quad (255)$$

$$\dot{Y}_1 = -Y_1 - rX_1 - Z(X_1 + X_2) \quad (256)$$

$$\dot{\bar{Y}}_1 = -\bar{Y}_1 - r\bar{X}_1 - Z(\bar{X}_1 + \bar{X}_3) \quad (257)$$

$$\dot{Y}_1 = \frac{19}{3}Y_2 - rX_2 - ZX_2 \quad (258)$$

$$\dot{\bar{Y}}_2 = \frac{19}{3}\bar{Y}_2 - r\bar{X}_2 - Z\bar{X}_2 \quad (259)$$

$$\dot{V} = -\frac{8}{3}L(V - \psi Z) + (X_1.U_1 + X_2.U_1 + X_1.U_2) \quad (260)$$

$$\dot{U}_1 = -L(U_1 - \psi Y_1) + \pi RX_1 + - V(X_1 + X_3) \quad (261)$$

$$\dot{\bar{U}}_1 = -L(\bar{U}_1 - \psi \bar{Y}_1) + \pi R\bar{X}_1 - V(\bar{X}_1 + \bar{X}_3) \quad (262)$$

$$\dot{U}_2 = -L(\frac{19}{3}U_2 + \frac{19}{3}\psi Y_2) - \psi RX_2 - X_2V \quad (263)$$

$$\dot{\bar{U}}_2 = -L(\frac{19}{3}\bar{U}_2 + \frac{19}{3}\psi \bar{Y}_2) - \psi R\bar{X}_2 - \bar{X}_2V \quad (264)$$

5.7 The extended Galerkin model with impermeable boundary conditions

A refinement of the fourteen-mode model is achieved by projecting the basic equations onto a subspace of the general Galerkin model that takes into account impermeability (see Linz and Lucke 1986 for the eight mode problem) at the horizontal boundaries. Refining still further by including rigidity is not possible as a closed form solution is not known, in short a boundary layer has to be put in. As the diffusive concentration current is proportional to $\nabla\xi$, where $\xi = c - \psi\theta$ is the diffusive current, then this quantity must vanish identically at the horizontal boundaries. Instead of choosing the modes given in chapter 4, equation (135) we identify the

following modes as being relevant:

$$w = X_1(t)sin\pi zcosk_c x + X_2(t)sin3\pi zcosk_c x \quad (265)$$

$$\theta = Y_1(t)sin\pi zcosk_c x + Y_2(t)sin3\pi zcosk_c x + Z(t)sin2\pi z \quad (266)$$

$$\xi = U_1(t)cosk_c x + U_2(t)cos2\pi zcosk_c x + V(t)sin\pi z \quad (267)$$

We notice that the equation for ξ will automatically satisfy the impermeability criterion, which may be written concisely as $\frac{d\xi}{dz} = 0$ at $z = 0, 1$.

The basic equations of motion expressed in terms of concentration, temperature and vertical velocity may be easily transformed so that the concentration current variable ξ replaces the concentration variable,c. The result of using, $\xi = c - \psi\theta$, gives

$$(\frac{\partial}{\partial t} - L\nabla^2)\xi + \psi\nabla^2\theta = -(v.\nabla)\xi. \quad (268)$$

$$(\frac{\partial}{\partial t} - \nabla^2)\theta - R_T w = -(v.\nabla)\theta. \quad (269)$$

$$\nabla^2(\frac{\partial}{\partial t} - \sigma\nabla^2)w = \sigma\nabla_1^2((1+\psi)\theta + \xi) - \nabla^2(v.\nabla)w. \quad (270)$$

The procedure for producing a truncation scheme is the same as given in section 5.4. However, their derivation is not quite so straightforward as outlined in section 5.4.. Recall, when performing a Galerkin truncation scheme with permeable boundaries we simply equated terms of that form, as orthogonality would automatically eliminate all other terms. With the impermeable boundary conditions this assertion is not so clear cut. Instead,

a number of integrals have to be determined. a table of those relevant integrals is given in appendix 4. The fourteen equations take the form:

$$\dot{X}_1 = -\sigma\frac{(\pi^2+k_x^2)}{3\pi^2}2X_1 + \frac{\sigma 3k_x^2}{(\pi^2+k_x^2)}((1-\psi)Y_1 -$$
$$+ \frac{\sqrt{28}}{\pi^2}U_1 - \frac{\sqrt{28}}{3\pi^2}U_3) \quad (271)$$

$$\dot{X}_2 = -\sigma\frac{((3\pi)^2+k_x^2)}{3\pi^2}2X_1 + \frac{\sigma k_x^2}{((3\pi)^2+k_x^2)}(3(1+\psi)Y_1$$
$$+ \frac{\sqrt{28}}{\pi^2}U_1 - \frac{\sqrt{29.8}}{5\pi^2}U_3) \quad (272)$$

$$\dot{Z} = -\frac{8}{3}Z + \sqrt{2}(X_1Y_1 + X_2Y_1 + X_1Y_3) \quad (273)$$

$$\dot{Y}_1 = -\frac{(\pi^2+k_x^2)}{3\pi^2}2Y_1 - rX_1 - Z(X_1+X_3) \quad (274)$$

$$\dot{Y}_2 = \frac{((3\pi)^2+k_x^2)}{3\pi^2}2Y_2 - rX_2 - \frac{ZX_2}{\sqrt{2}} \quad (275)$$

$$\dot{V} = -\frac{8}{3}LV - L16/9\psi Z) - \frac{1}{3}(X_1U_1) \quad (276)$$

$$\dot{U}_1 = -L\frac{k_x^2}{3\pi^2}2U_1 - \frac{(\pi^2+k_x^2)}{3\pi^2}2\psi Y_1 + RX_1 + \frac{VX_1}{2} \quad (277)$$

$$\dot{U}_2 = -L(\frac{19}{3}U_2 + \frac{19}{3}\psi Y_2) - \psi RX_2 - X_2V, \quad (278)$$

together with the equations for the conjugate variables $\dot{X}_1$, $\dot{X}_2$ $\dot{Y}_1$, $\dot{Y}_2$, $\dot{Y}_1$, $\dot{Y}_3$. The form of the advective contribution changes from the permeable model, details are given in appendix 4. We have used the scalings:

$$\frac{\sqrt{3}\pi}{\sqrt{2}}X_1 \longrightarrow X_1 \quad (279)$$

$$\frac{\sqrt{3}\pi}{\sqrt{2}}X_2 \longrightarrow X_2 \quad (280)$$

$$\frac{27\pi^3\sqrt{2}}{sqrt34}Y_1 \longrightarrow Y_1 \quad (281)$$

$$\frac{27\pi^3\sqrt{2}}{sqrt34}Y_2 \longrightarrow Y_2 \tag{282}$$

$$\frac{-27\pi^3}{\sqrt{24}}Z \longrightarrow Z \tag{283}$$

$$\frac{\sqrt{2}27\pi^2 V}{2} \longrightarrow V \tag{284}$$

$$\frac{27\pi^2}{\sqrt{3}}U_1 \longrightarrow U_1 \tag{285}$$

$$\frac{27\pi^2}{\sqrt{3}}U_2 \longrightarrow U_2, \tag{286}$$

rescaling time as before.

5.8 Invariant subspaces

Before we discuss the dynamics of the models it is instructive to look at any invariant subspaces that may exist in the truncated models. The O.D.E.'s have two invariant subspaces: this reflects the physical symmetries of the flow. If we set those modes that are conjugate to X_1, X_2, Y_1, Y_2, U_1, U_2, to zero then the flow remains in that subspace hence, we obtain a legitimate subspace. Therefore, the dynamics of the fourteen mode model has a subspace whose dynamics are of those of the eight model model.

Are the dynamics of the eight-mode Cross model also included as an invariant subspace in the fourteen mode model? As the Cross truncation is not an invariant subspace of the full fourteen mode model, it would seem no. This is precisely why Cross observes that numerically an arbitrarily small perturbation will destroy the period doubled state observed by Knobloch et al at critical parameters (R,ψ)= (r$_4$,-4α) in the five mode model.

5.9 Linear theory

5.9.1 Pitchfork bifurcation

Let us analyse some aspects of the dynamics of the truncation scheme. It is straightforward to show that the linear theory for equation (251-264) for the stationary bifurcation is equivalent to that presented in chapter 3. To do so, we assume X_s, Y_s, Z, U_s, V. are small and we linearise as usual. This gives a matrix equation

$$\dot{w} = L(w), \tag{287}$$

for linear stability, we obtain a condition on the eigenvalues, given by $det(I\lambda - L(w)) = 0$. Three blocks of the determinant decouple to produce

$$\begin{vmatrix} \lambda+\sigma & -\sigma & -\sigma \\ -r & (1+\lambda) & 0 \\ -\psi r & -\psi L & (L+\lambda) \end{vmatrix} = 0 \tag{288}$$

$$\begin{vmatrix} \lambda+\frac{19}{3}\sigma & -\frac{3}{19}\sigma & -\frac{3}{19}\sigma \\ -r & (\frac{19}{3}+\lambda) & 0 \\ -\psi r & -\frac{19}{3}\psi L & (\frac{19}{3}L+\lambda) \end{vmatrix} = 0 \tag{289}$$

$$\begin{vmatrix} \lambda+\frac{8}{3} & 0 \\ \frac{8}{3}\psi L & \frac{8}{3}L+\lambda \end{vmatrix} \tag{290}$$

for the stationary 8-mode permeable model. The expressions given in the above equations produce two cubic and one quadratic equation. To find the threshold for stationary convection, we demand $\lambda_1 = 0$ in equation (288). This results in the condition that the constant term from equation (288)

be zero. The reduced critical Rayleigh number is,

$$r_s = \frac{1}{(1+\psi+\frac{B}{L})}, \tag{291}$$

identical to the result obtained in (3.1) in reduced variables, with critical horizontal wave number $k_m = \frac{\pi}{\sqrt{2}}$. To show the other eigenvalues at criticality is straightforward. For the fourteen mode impermeable model (equations 263-278) the relevant decoupled determinant is:

$$\begin{vmatrix} \lambda+\sigma(\frac{k_x^2+\pi^2}{\frac{B}{L}} & -(1+\psi)\frac{k_x^2\pi^2}{\frac{B}{L}(k_x^2+\pi^2)}\sigma & -\frac{8}{\pi^2}\frac{k_x^2\pi^2}{\frac{B}{L}(k_x^2+\pi^2)}\sigma \\ -r & (\frac{k_x^2+\pi^2}{\frac{B}{L}}+\lambda) & 0 \\ 0 & -\frac{k_x^2+\pi^2}{\frac{B}{L}}\psi & (\frac{k_x^2+\pi^2}{3}\frac{B}{2}L+\lambda) \end{vmatrix} = 0. \tag{292}$$

This corresponds to equation (82) of the permeable model and gives the stationary critical values:

$$r_{st} = \frac{(\pi^2+k_x^2)k_x^4}{3q^2(1+\psi+\frac{8.2\pi^2q}{\pi^2\frac{B}{L}k^2})}. \tag{293}$$

The critical value of $r = r_s$, the reduced Rayleigh number is found by equating the constant terms to zero. By evaluating $\frac{dr_s}{dk} = 0$, we obtain the critical wave number;

$$k_m = \frac{(1+\psi)L - \frac{16}{\pi^2}\psi}{(1+\psi)L + \frac{2}{\pi^2}\psi} \tag{294}$$

The corresponding stability curves are given in figure 9.

5.9.2 Hopf bifurcation

Similarly, the Hopf bifurcation is found when a pair of complex conjugate roots of the eigenvalue equation (286), cross the imaginary axis (assuming

for the moment that certain transversality conditions hold). We find

$$r_{c0} = \frac{(1+L)(1+L+\sigma+\frac{L}{\sigma})}{(1+\sigma+\sigma\psi)}. \tag{295}$$

The condition that the Hopf frequency be real places a condition on the separation ratio:

$$\psi < \frac{-(1+\sigma)L^2}{(L^2+\sigma L^2+L+\sigma L+\sigma)}. \tag{296}$$

These results are confirmed by Cross (1986).

5.9.3 Tricritical bifurcation

The tricritical bifurcation is realised by studying the equations in the vicinity of (r_c, ψ_t), with

$$\psi_t = \frac{-L^2}{(1+L+L^2+L^3)}. \tag{297}$$

A few representative values of the stress parameters are shown in figure 13. The unstable branches depicted by the broken lines are located by choosing an initial condition and following its evolution. If it evolves to the upper stable branch then it is above the unstable solution, alternatively below the unstable branch the flow will relax to the zero solution.

5.9.4 Broken tricritical state

The broken tricritical state may be realised by adding a constant forcing term, C, to the model equations. In such a way we may phenomenologically

introduce a symmetry broken state. Equation (249) becomes

$$\dot{X}_1 = -\sigma(X_1 - Y_1 - U_1) + C \tag{298}$$

For illustrative purposes the constant, C= 0.0001. Its effect is sought numerically. The bifurcation diagram corresponding to this value of C is given in figure 7. For a small amplitude set of starting values, with X chosen to positive, we occupy the top branch at A. As we reduce r we jump at B. A jump at C is seen only if a sufficiently small value of X is used (below branch D), when decreasing r. The branch for negative values of X is located by choosing sufficiently large negative values of X, below the unstable branch at E.

In an experiment, if the temperature difference is varied smoothly for a fixed separation ratio, from quiesence, a jump is seen at C, if the model is correct and a symmetry breaking bifurcation is present. The top branch corresponds to roll rotating in a clockwise direction say. The bottom branch would correspond to the cell rotating in the opposite sense.

5.10 Some basic properties of the truncation schemes

Neglecting the modes X_2, Y_2, U_2 reduces the fourteen mode description to eight modes. Removing the complex conjugate contributions (the hatted variables) reduces the eight to five equations and to the Moore model. In the limit of negligible concentration gradient and vanishing separation ratio the model becomes that of Lorenz.

It was shown by Cross that the standing waves were unstable to travelling wave perturbations in large aspect ratio cells. This was revealed by Cross's eight mode model. This scenario was later revealed, by experiment, to be true. Figure 10 shows results of onset of the Hopf bifurcation for the eight mode model; see Kolodner (1986) for the experimental data. Notice there is a large amplitude non-linear saturation even very near criticality. The Cross model is, however, incomplete as the addition of further modes stabilise the travelling wave. Figure 11 demonstrates this quite well.

The natural question to ask is how much of this behaviour is seen in experimentation? If we concentrate for the moment on the Hopf bifurcation it has been observed by Kolodner et al that the travelling wave state is associated with a subcritical bifurcation. Recall, the theory based on free-slip permeable boundary conditions predicts a supercritical bifurcation. This is exactly the reason the extended fourteen mode model has been derived as it allows the subcritical Hopf bifurcation.

In summary, therefore, the fourteen mode model seems to get the most dynamics right. It was our lack of understanding of the degeneracies and symmetries implicit in binary fluid mixtures that meant all previous models were in some respect inadequate, even at the critical bifurcation point.

5.11 Far from criticality

Far from criticality, away from onset of both the stationary and oscillatory instabilities. we assume the legitimacy of the truncation scheme breaks

down. To what extent it breaks down is unclear.

What are the dynamics in this more general regime and do they have any relevance to what is observed in experiment? This is too general a question to possibly answer in totality, as we would expect to observe spatial irregularities. In a carefully controlled experiment, in which we have a small aspect ratio cell together with a low Prandtl number fluid Libchaber (1972) discovered that the aperiodicity Lorenz had found was indeed observable, at least at a qualitative level.

The same conclusions could be said to be relevant for binary fluids, as the five mode model yields a similar route to chaos, through a period doubling sequence. The global results of the fifth order system can be summarised schematically by fig (13) reproduced from fig(3) of Moore et al. The fifth order system supports a heteroclinic explosion (Moore et al), for parameter values $(R, \psi) = (8, 81, -1.16)$. The Sh ilnikov mechanism, in which flow is reinjected near an unstable equilibrium together with a condition on the eigenvalues, provides a sufficient mechanism for chaotic dynamics. In the eight mode model this mechanism is suppressed.

For the eight mode Cross model the behaviour is relatively straightforward. Beyond the Hopf bifurcation point two stable limit cycles bifurcate from the quiesent state. The two limit cycles become unstable and bifurcate to unstable tori; this appears as a rather uninteresting spiraling to a fixed point. The bifurcation can be confirmed using Floquet theory.

Chapter 6 - Conclusions

Conclusions

The possibility of predicting fluid motion is an intriguing subject.

In simple geometries we have a strong grasp of the correspondence between the P.D.E's that govern the fluid's motion and bifurcation theory, which attempts to classify qualitative changes in the solutions of the P.D.E's.

In chapter 1 we present the model equations of motion for convection in a two dimensional layer of perfectly miscible binary fluid. The equations are derived from various conservation principles.

In chapter 2 we draw upon dynamical systems theory to provide a setting to study the model problem of chapter 1. The Lorenz model is used to demonstrate various aspects of the theory.

The tricritical bifurcation describing the transition between a forward and backward pitchfork bifurcation occurs generically in codimension-2 systems with Z_2 (reflectional) symmetry. The tricritical bifurcation is investigated using the method of multiple scales. A prediction of coefficients of the normal form is given. The results are compared with the available experimental data of Gao and Behringer 1986. Chapter 3 concludes with a discussion of the broken tricritical state.

The Hopf bifurcation is discussed in detail in chapter 4. The overall

symmetry present is $O(2) \times S^1$, the spatial reflections and rotations of the circle together with the phase shift symmetry S^1. It gives rise to a degenerate Hopf bifurcation. It is degenerate in the sense that a fifth order description is required to describe it. A normal form is derived for the pure travelling wave state.

In Chapter 5 a number of Galerkin truncation schemes are investigated. They are constructed to include these higher order bifurcation phenomena. The tricritical and degenerate Hopf bifurcations are treated consistently within a model. The equations are improved upon by projecting the 14-modes onto a more appropriate subspace.

The prediction of coefficients in amplitude equations given in Chapters 3 and 4 is derived using reductive perturbation theory. The more general theory treating the finite dimensional problem with $O(2)$ symmetry is an excellent general framework, but is lacking in its predictive power.

Appendix 1

6.1 Derivation of continuity equation for mass

Let c be the concentration of one component i be the flux of concentration c by diffusion. Then, we may equate the rate of change of the amount of that component to the amount transported by the motion of the fluid and diffusion. Therefore;

$$\int_V \rho c dV = -\int_{\partial V} \rho c \vec{V}.d\vec{S} - \int_{\partial V} i.d\vec{S} \tag{299}$$

We can rewrite this in differential form using Gauss' Law to give,

$$\rho(\frac{\partial c}{\partial t} + \vec{V}.\nabla c) = -\nabla.i. \tag{300}$$

6.2 Conservation of energy

In this section we aim to derive an equation for the temperature, T in the same spirit as in the derivation of the equation for the concentration. We achieve this by using conservation of energy for the system. If we calculate the rate of change of the energy per unit volume this may be equated to the divergence of the total energy flux, as the total energy of the fluid is conserved. The energy per unit volume is:

$$(\frac{1}{2}\rho v^2 + \rho\epsilon), \tag{301}$$

where ϵ is the internal energy per unit mass. Before we can calculate the rate of change of energy per unit volume in the required variables of

temperature and concentration we need two thermodynamic relations:

$$d\epsilon = TdS + \frac{P}{\rho^2}d\rho + \mu dc \tag{302}$$

$$dw = TdS + \frac{1}{rho}dP + \mu dc. \tag{303}$$

where μ is the chemical potential of the mixture, P, the pressure, T, the temperature, S, the entropy and ϵ, w , the internal energy and the heat function per unit mass. We use these relations to write the rate of change of energy per unit mass as:

$$\frac{\partial}{\partial t}(\frac{1}{2}\rho v^2 + \rho\epsilon) = -\nabla.[\rho\vec{V}(\frac{1}{2}V^2 + w) \quad - \quad \vec{V}.\sigma' + q] \tag{304}$$

$$+\rho \quad T \quad (\frac{\partial S}{\partial t} + \vec{V}.\nabla S) + \nabla q - \mu\nabla i \tag{305}$$

where σ' is the stress tensor. Conservation of energy requires that,

$$\frac{\partial}{\partial t}(\frac{1}{2}\rho v^2 + \rho\epsilon) = -\nabla.[\rho\vec{V}(\frac{1}{2}V^2 + w) - \vec{V}.\sigma' + q]. \tag{306}$$

Hence,

$$\rho T(\frac{\partial S}{\partial t} + \vec{V}.\nabla S) + \nabla q - \mu\nabla i = 0. \tag{307}$$

In its derivation we have used the Navier-Stokes equation and have implicitly neglected a term proportional to a derivative of the velocity, which takes into consideration heating effects due to the motion of the fluid. Notice that equation (307) is expressed in terms of the more favourable thermodynamic quantity, the entropy. We may relate S to T and c by the following identity:

$$\frac{\partial S}{\partial t} = \frac{C_p}{T}\frac{\partial T}{\partial t} - (\frac{\partial \mu}{\partial T})\frac{\partial c}{\partial t}. \tag{308}$$

Finally, using equations (307) and (308) we obtain:

$$\rho C_p \frac{DT}{Dt} = \nabla.(q - \mu i). \tag{309}$$

The intermediate steps in the derivation outlined above are given more fully in Landau and Lifshitz (L.L.)(pg 130).

6.3 Diffusive fluxes

In making the approximation that the concentration and temperature gradients are small it seems altogether reasonable to assume that the fluxes i and q may be expressed in terms of a linear combination of gradients. Invoking Onsager reciprocal relations or as L.L. put it, a symmetry principle, we can relate some of the coefficients. After changing variables the equations for i and q are:

$$i = -\rho D[\nabla c + (k_T/T)\nabla T] \tag{310}$$

$$q = [k_T(\partial\mu/\partial c)_{p,t} + \mu]i - \kappa\nabla T \tag{311}$$

where, D is the diffusion coefficient, $\kappa = k_T D$ is the thermal diffusion coefficient, k_T is the thermal diffusion ratio.

6.4 Putting it all together

By making use of the previous two subsections we can write out the equations for the concentration and temperature explicitly by elimination of i

and q from the equations. Performing this simplification we obtain:

$$\frac{\partial c}{\partial t} - \vec{V}.\nabla c = D[\Delta c + (k_T/T)\Delta T] \tag{312}$$

$$\frac{\partial T}{\partial t} - \vec{V}.\nabla T = (k_T/C_p)(\partial \mu/\partial c)_{p,T}\frac{Dc}{Dt} + \kappa \Delta T. \tag{313}$$

Hence, together with the equation for the velocity field the problem is completely prescribed. As a general observation it must be realised that the equations are valid only when the physical coefficients may be regarded as constant with respect to the temperature and concentration. The origin of this simplification in these cases is due to the smallness of the coefficient of volume expansion. However, any deductions we may make in this respect must be treated with some caution.

6.5 The non-dimensionalisation

Non-dimensionalisation of the equations involves extracting out characteristic collections of the physical parameters into non-dimensional parameters groups. This process is by no means unique. By choosing parameter groups (or numbers) that leave the equations looking as simple as possible we generally arrive at the same characteristic numbers that arise in similar problems. The scaling used in the derivation of equations (13), (14) and (15) of section 1 are as follows:

$$\frac{\partial}{\partial t} \longrightarrow \frac{D_T}{d^2}\frac{\partial}{\partial t} \tag{314}$$

$$\Delta \longrightarrow \frac{\Delta}{d^2} \tag{315}$$

$$w \longrightarrow \frac{D_T}{d} w \tag{316}$$

$$\theta \longrightarrow \frac{\nu D_T}{\alpha g d^3} \theta \tag{317}$$

$$c \longrightarrow \frac{\nu D_T}{\beta g d^3} c \tag{318}$$

with the characteristic parameters given by:

$$R = \frac{g d^4 \alpha \beta}{\nu D_T} \tag{319}$$

$$L = \frac{D}{D_T} \tag{320}$$

$$\psi = \frac{-\beta k_T}{\alpha T} \tag{321}$$

$$\sigma = \frac{\nu}{D_T} \tag{322}$$

APPENDIX 2

Critical Rayleigh number

From the condition

$$|Lw_0| = \begin{vmatrix} k^4 & -(1+\psi)k_a^2 & \psi k_a^2 \\ R & -k^2 & -LAk^2 \\ 0 & -k^2 & -L(1+A)k^2 \end{vmatrix} \tag{323}$$

$$= k^4(Lk^4) - (1+\psi)k_a^2 RL(1+A)k^2 - Rk^2\psi k_a^2 = 0 \tag{324}$$

Rearranging,

$$R_c = \frac{k^6}{k_a^2((1+\psi)(1+A)+\frac{\psi}{L})} \qquad , k^2 = k_a^2 + k_z^2. \tag{325}$$

Critical k_z

For minimum R:

$$\begin{aligned} \frac{dR}{d(k_a^2)} &= 3(k_a^2+\pi^2)^2 k_a^{-2} - (k_a^2+\pi^2)^3 k_a^{-4} \qquad (326) \\ &= \frac{(k_a^2+\pi^2)^2)^2}{k_a^2}(3 - \frac{(k_a^2+\pi^2))^2}{k_a^2}) \\ &= 0. \end{aligned}$$

Therefore,

$$k_a^2 = \frac{\pi^2}{2} \tag{327}$$

Appendix 3

This contains the integrals required to evaluate the impermeable Galerkin model.

For the pervious model the following will be useful:

$$sin(A+B) = sinAcosB + cosAsinB \tag{328}$$

$$sin(A-B) = sinAcosB - cosAsinB \tag{329}$$

$$cos(A-B) = cosAcosB - sinAsinB \tag{330}$$

$$cos(A-B) = cosAcosB + sinAsinB \tag{331}$$

Impermeable free-slip boundary conditions ($D\xi = 0$)

We define.

$$< f,g >= \int_0^{\frac{\pi}{a}} f dz \left(\int_0^z\right) g dz. \tag{332}$$

In this appendix we compute the relevant integrals for the Galerkin truncation projected onto an impermeable subspace (that is $D\xi = 0$ replaces $c = 0$ at the horizontal boundaries). The equations of motion are:

$$\left(\frac{\partial}{\partial t} - L\nabla^2\right)\xi + \psi\nabla^2\theta = -(v.\nabla)\xi, \tag{333}$$

$$\left(\frac{\partial}{\partial t} - \nabla^2\right)\xi - R_T w = -(v.\nabla)\theta, \tag{334}$$

$$\nabla^2\left(\frac{\partial}{\partial t} - L\nabla^2\right)w = \sigma\nabla_3^2((1+\psi)\theta - \xi) - \nabla^2(v.\nabla)w. \tag{335}$$

We choose the following modes for the velocity w and u. temperature θ and ξ.

$$w = X sin\pi z cosk_a x + F sin3\pi z cosk_a x, \tag{336}$$

$$u = -\frac{\pi}{k_a} X sin\pi z cosk_a x - \frac{3\pi}{k_a} F sin3\pi z cosk_a x, \tag{337}$$

$$\theta = Y sin\pi z cosk_a x + Z sin2\pi z + G sin3\pi z cosk_a x, \tag{338}$$

$$\xi = U cosk_a x + V cos\pi z + H cosk_a x cos\pi z. \tag{339}$$

The advective forcing takes the form:

$$\begin{aligned} w\partial_z\xi + u\partial_x\xi &= \frac{\pi}{2}[XV cosk_a x \\ &+ (FV - XV) cos2\pi z cosk_a x - FV cos4\pi z cosk_a \\ &+ XU cos\pi z(1 - cos2k_a x) + 3UF cos3\pi z(1 - cos2k_a x) \\ &- HX cos(n-1)\pi z(1 - (n-1)(1 + cos2k_a x) \\ &+ HX cos(n+1)\pi z(1 - (n+1)(1 + cos2k_a x) \\ &+ HF cos(n-3)\pi z(3 + (n-3)(1 + cos2k_a x) \\ &+ HF cos(n+3)\pi z(3 - (n+3)(1 + cos2k_a x)]. \end{aligned} \tag{340}$$

$$\begin{aligned} w\partial_z\theta + u\partial_x\theta &= \frac{\pi}{2}[XY cos2\pi z \\ &+ GX sin2\pi z(1 - 2(cos2k_a + 1)) + YF sin2\pi z(1 - 2(1 - cos2k_a)) \\ &+ GX sin4\pi z(1 + (cos2k_a + 1)) + YF sin4\pi z(1 + (1 - cos2k_a)) \\ &+ 3GF sin6\pi z - 2ZX sin3\pi z cosk_a x - 2ZX sin\pi z cosk_a x \\ &+ 3GF sin6\pi z + 2ZF sin5\pi z cosk_a x - 2ZF sin\pi z cosk_a x] \end{aligned} \tag{341}$$

The following integrals are important: for the $cosk_n x$ mode:

$$< cos^2 k_n x >= \frac{\pi}{2k_n}, \tag{342}$$

$$< cosn\pi z cos^2 k_n x >= 0, \tag{343}$$

$$< cosn\pi z cosk_n x >= 0, \tag{344}$$

The $cos\pi z$ mode:

$$< cos2\pi z cos\pi z cosk_n z >= 0, \tag{345}$$

$$< cos^2 \pi z >= \frac{\pi}{k_n}, \tag{346}$$

$$< cos^2 \pi z cos2k_n x >= 0, \tag{347}$$

$$< cos3\pi z cos\pi z >= 0. \tag{348}$$

The $sin2\pi z$ mode:

$$< sin^2 2\pi z >= \frac{1}{2}. \tag{349}$$

The $sin\pi z cosk_n x$ mode:

$$< sin^2 \pi z cos^2 k_n x >= \frac{\pi}{4k_n}. \tag{350}$$

The $sin3\pi z cosk_n$ mode:

$$< sin^2 3\pi z cos^2 k_n x >= \frac{\pi}{4k_n}, \tag{351}$$

$$< sin3\pi z cos^2 k_n x >= \frac{1}{3k_n}, \tag{352}$$

$$< sin3\pi z cos2\pi z cos^2 k_n x >= \frac{3}{5k_n}, \tag{353}$$

$$< cos4\pi z sin3\pi z cos^2 k_n x >= -\frac{3}{7k_n}. \tag{354}$$

Appendix 4

Implicit function theorem

Let $\mathbf{y} \in \mathbf{R}^n$ with the usual Euclidean vector norm. The equation:

$$\underline{0} = \mathbf{f}(\mathbf{y}, \lambda), \tag{355}$$

with $\lambda \in R$, $f(\mathbf{y}, \lambda) \in \mathbf{R}^n$; $\underline{0}$ stands for the zero vector. In general, the equation $\underline{0} = \mathbf{f}(\mathbf{y}, \lambda)$ defines implicitly one or more curves in $(1+n)$-dimensional $(\mathbf{y}, \lambda)$ space.

The general assertion is as follows:

(1) $f(\mathbf{y}_0, \lambda_0) = \underline{0}$

(2) f is continuously differentiable on its domain,

(3) $D_y f(\mathbf{y}_0, \lambda_0)$ is non-singular.

Then there is an interval $\lambda_1 < \lambda_0 < \lambda_2$, in which a function $\mathbf{y} = \mathbf{F}(\lambda)$ defined by $\underline{0} = \mathbf{f}(\mathbf{y}, \lambda)$ with the following properties holding for all λ with $\lambda_1 < \lambda < \lambda_2$:

a) $f(F(\lambda), \lambda) = 0$,

b) $F(\lambda)$ is unique with $\mathbf{y}_0 = \mathbf{F}(\lambda_0)$,

c) $F(\lambda)$ is continuously differentiable,

d) $D_y f(\mathbf{y}, \lambda)\frac{d\mathbf{y}}{d\lambda} + \mathbf{f}_\lambda(\mathbf{y}, \lambda) = \mathbf{0}$.

Appendix 5

Codimension-2

The codimension-2 point occurs when the Rayleigh number R, and the separation ratio ψ are chosen such that the Hopf and steady bifurcations are coincident. This occurs when:

$$\psi_{CT} = -\frac{L^2(1+\sigma)}{L(1+L)(1+\sigma)+\sigma} \tag{356}$$

and

$$R_{CT} = \frac{27}{4}\pi^4(1+\frac{L}{\sigma}(1+L)(1+\sigma)). \tag{357}$$

These estimates are not in complete agreement with the experimental results of Sullivan and Ahlers (1988) - the idealised boundary conditions used are considered to be the root cause.

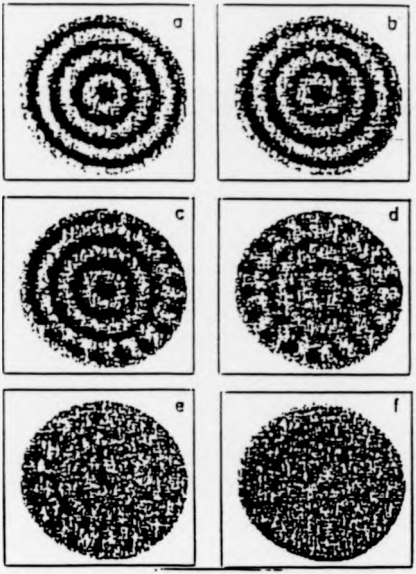

Figure 1.

A single fluid in a cylindrical dish heated from below. Flow patterns at several values of ϵ, taken from V. Steinberg et al.(1985). The values of ϵ are (a) 0.29; (b) 0.15; (c) 0.13; (d) 0.08; (e) 0.02; (f) -0.06. Patterns a and b represent concentric flow. For the rest, except (f) the concentric flow is unstable, but the evolution of the pattern is slow and images do not represent a steady state. This figure demonstrates the phenomena of critical slowing down near the point of bifurcation.

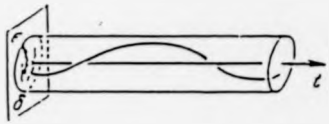

Figure 2.
A stable equilibrium

Figure 3.
An asymptotically stable flow

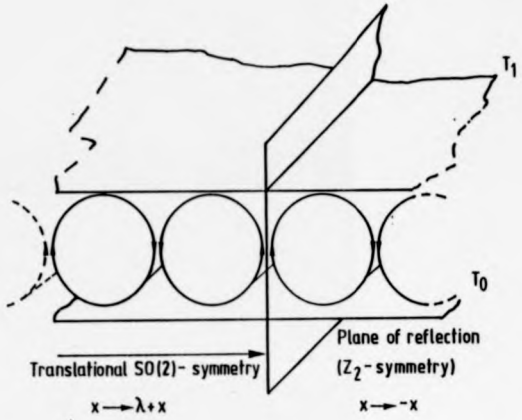

Figure 4.
The roll configuration in a layer of fluid. The various symmetries are shown.

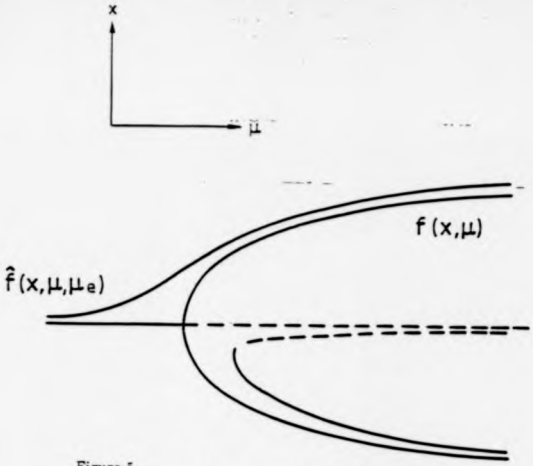

Figure 5.
The pitchfork and broken pitchfork bifurcations.

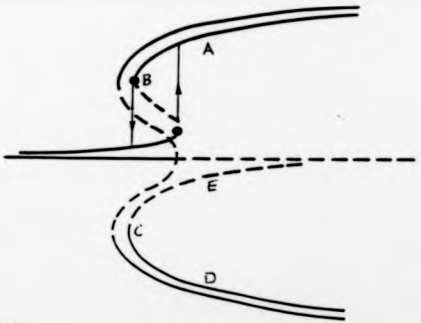

Figure 7.
The interlocal bifurcation. The arrows indicate the hysteretic phenomena

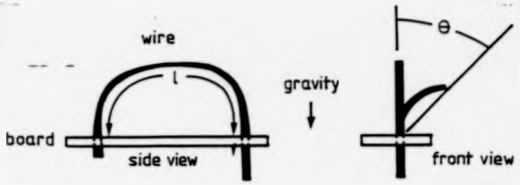

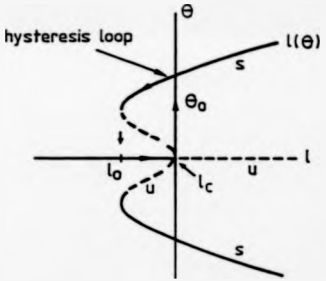

Figure 6.
Benjamin's apparatus for demonstrating the buckling of a viscoelastic arch of wire (taken from D.D. Joseph (1983)).

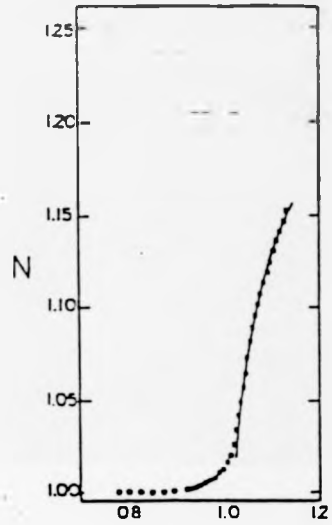

Figure 8.
Nusselt number versus the reduced Rayleigh number. The solid curve satisfies $Nu - 1 = (\frac{\epsilon}{0.22})^{2.5}$. Data taken from Gao and Behringer 1988.

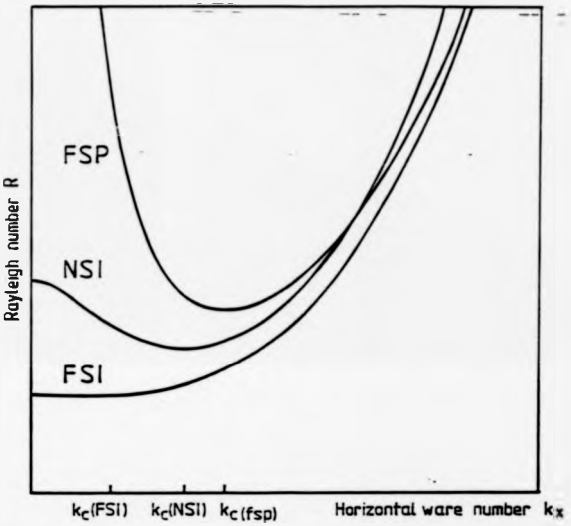

Figure 9.

The stability curves (Rayleigh number versus wave number) for the free slip permious (FSP), no slip impermious (NSI) and free slip impermious (FSI). The critical horizontal wave numbers are shown.

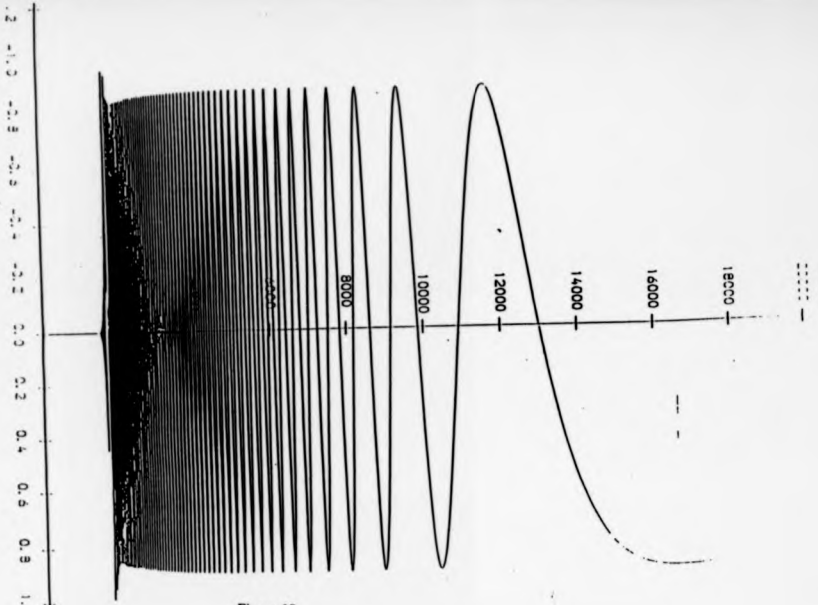

Figure 10.

X versus time at onset of convection for the eight mode problem. It shows the characteristic precipitious relaxation to the oscillatory state. This state becomes unstable to a fixed point.

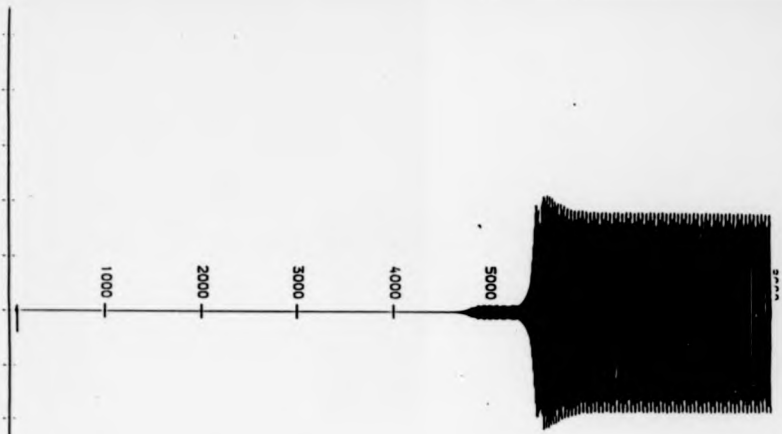

Figure 11.
X versus time for the fourteen mode problem, the final oscillatory state is stable.

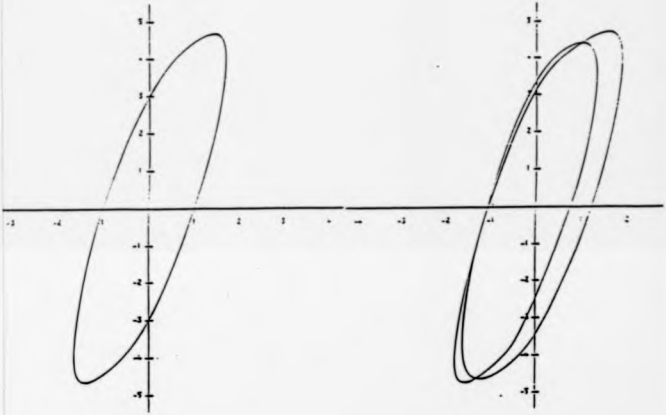

Figure 12.

X_1 versus Y_1 for the five mode model before and after the period doubling bifurcation.

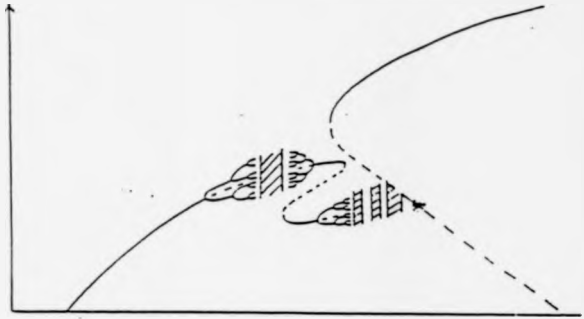

Figure 13.
Schematic representation of the period doubling cascade to the heteroclinic explosion (Moore et al 1983).

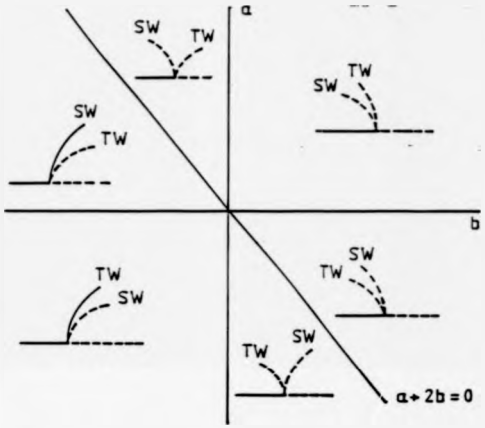

Figure 14.

Bifurcation diagram (A vs. λ) in the a,b) plane, taken from Knobloch et al. (1986). Solid lines denote stable solutions, dashed lines indicate unstable solutions.

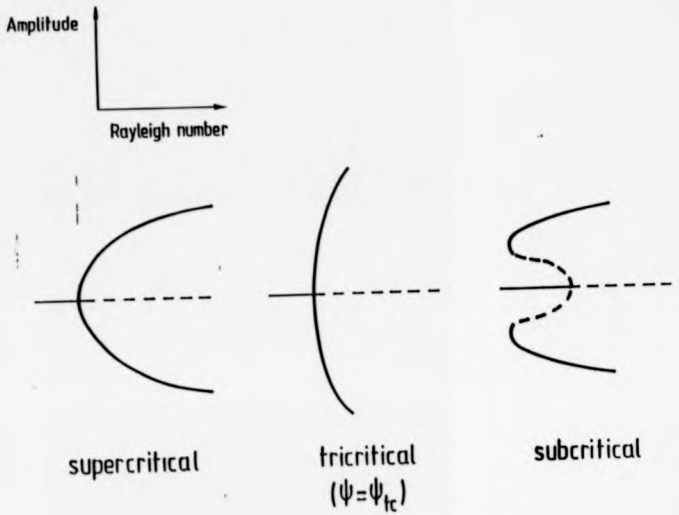

Figure 15.
Bifurcation diagram showing supercritical ($\psi > \psi_c$), tricritical ($\psi = \psi_c$) and subcritical($\psi < \psi_3$) behaviour.

References

[1] AHLERS G, and BEHRINGER Phys. Rev. Lett 40 712 (1978)

[2] AHLERS G., HOHENBERG P.C., LUCKE M., Phys Rev A 32 6 (1985)

[3] AHLERS G., LUCKE M., preprint Phys Rev A. (1986)

[4] AHLERS G., Phys Rev Lett 24 1333-1336

[5] ARNOLD V.I. Ordinary Differential Equations (1981) MIT press, ARNOLD V.I. Funct. Anal. Appl. 11, 1 (1984)

[6] BENJAMIN T.B. Proc. R. Soc. Lond. A 359 27-43 (1978)

[7] BENJAMIN T.B. and MULLIN T. J. Fluid Mech 121 219 (1982)

[8] BRAND H.R. and STEINBERG V., Phys. Lett. 93A, 333 (1983) , BRAND H. Physica 119a 327 (1983), BRAND H.R. and STEINBERG V., Physica 119A. 327 (1983) , BECK J.L. Phys of Fluids 15 8 (1972) 1377-1383

[9] BUSSE F.H., Rep Prog Phys. 41, 1929 (1978)

[10] CROSS M.C., Phys Letts A 119 1 (1986)

[11] CARR J. Applications of centre manifold theory, Springer-Verlag.

[12] CHANDRASEKAR S., Hydrodynamic and Hydromagnetic Stability (Oxford University, London, 1961; Dover 1981)

[13] DULLIEN F.A.L. Porous Medium, Fluid Transport and Pore Structure (Academic, New York, 1979)

[14] De GROOT and MAZUR Nonequilibrium thermodynamics 1961 North-Holland Amsterdam and FITTS nonequilibrium thermodynamics (1962) McGRAW HILL series in advanced chemistry

[15] FLOQUET G. Ann. Ecole Norm Ser 212 47 (1883)

[16] FRANCESCHINI V., TEBALDI C., J. Stat Phys 1 6 (1979)

[17] GAO H. and BEHRINGER R.P. (1986) Phys Rev A 34, 1501

[18] GALERKIN (1915) (See FINLAYSON B.A., The Methods of Weighted Residuals and Variational Principles (Academic Press, New York, 1972)

[19] GOLUBITSKY and STEWART I Arch Rat. Mech. Anal. 87 2 (1985) 107-165 also a for a better formulation of the theorem of Hopf with symmetry GOLUBITSKY M STEWART I and SCHAEFER D.G. Singularities and Groups in bifurcation theory Vol 2 App. Math. Series volume 60

[20] GUCKENHEIMER J. SIAM J. Math Anal. 15, 1 (1984)

[21] GUCKENHEIMER J. IEEE Trans. Circuits Syst. 27 982 (1980)

[22] GUCKENHEIMER J. KNOBLOCH E. Geophys Astrophys, Fluid Dynamics (1983) 23 247-272

[23] GUCKENHEIMER J. HOLMES P. Nonlinear Oscillations, Dynamical Systems and Bifurcations of Vector Fields Springer, New York, 1983.

[24] GUCKENHEIMER J. SIAM J Math Anal 15 1 (1984)

[25] GUTKOWICZ-KRUSIN, COLLINS M.A., ROSS J., Phys Fluids 22 1443 (1979)

[26] GUTKOWICZ-KRUSIN, COLLINS M.A., ROSS J., Phys Fluids 22 1451 (1979)

[27] HAKEN H. Laser theory, in Encyclopedia of Physics Vol xxv (1970) and PEPLOWSKI P. Physica 6D (1983) 364-374

[28] HIRSCH and SMALE S. Differential Equations Dynmical systems and linear algebra (Academic, NY 1974)

[29] HOHENBERG P.C., SWIFT J.B. Phys Rev A 35 9 (1987)

[30] HOLMES P.J. Physica 2D 449 (1981)

[31] HOLMES P.J. J. Sound Vib (1977) 53(4), 471-503

[32] HOPF E. Abezweg einer periodischen Lonsung von einer stationaren Lonsung eines Differentialsystems, Ber. Math-Phys. Sachsische Adademie der Wissenschaften Leipsig 94 (1942) 1-22

[33] HURLE D.T.J., JAKEMAN F., J. Fluid Mech. 47 667 (1971)

[34] JOSEPH D.D. Stability of Fluid Motion, Springer Tracts Nat Phil vols 27,28 (Springer, Berlin,Heidelberg, NY 1976)

[35] KADANOFF L. Phys Scripta T9 5-10 (1985)

[36] KOLODNER P., PASSNER A., WILLIAMS and SURKO C.M. Proceeding of int conference on the physics of chaos and systems far from equilibrium, Monterey California 10-14 Jan 1986 Nuc. Phys. B.

[37] KNOBLOCH E. Phys Rev A, 27 1 (1983)

[38] KNOBLOCH E. Phys. Fluids 23 1918 1980

[39] KNOBLOCH E. Geo Astro Fluid Dyn. 23 274 (1983) and ARMBRUSTER D. Physica 27D (1987) 433-439

[40] KNOBLOCH E., DEANE A.E. and TOOMRE J. (1987) Springer series in synergetics vol 37 Ed., GUTTINGER W and DANGELMAYR G.

[41] LADYZHENSKAYA O.A. Sov. Phys. Dokl. 17 (1973), 647

[42] LANGER Phys Scripta T9 119-122 (1985)

[43] LEE G., LUCAS P., TYLER A.. Phys Lett 75A 81 1979

[44] LEE G., LUCAS P., TYLER A..

[45] LINZ S.J. LUCKE M. Phys Rev A 35 9 (1987)

[46] LANDAU L.D. and LIFSHITZ E.M. , Fluid Mechanics (Pergammon, New York 1959)

[47] LORENZ E.N., J. Atm. Sci. 20 130 (1963) and RUELLE D., Quantum dynamics: models and mathematics. wien: springer1976)

[48] MAY R.B. Nature 261 459 (1976)

[49] MOORE D.R., TOOMRE J., KNOBLOCH E., WEISS N.O., Nature 303 5919 pp 663-667, HUPPERT H.E., and MOORE D.R., J. Fluid Mech. 78 821 1976, HUPPERT H.E., and MOORE D.R., J. Fluid Mech. 78 821 1976 and also ARARWAL A., BHATTACHARJEE J.K., BANERJEE K., Phys Rev B, 30 11 (1984).

[50] MARSDEN J. and McCRACKEN The Hopf bifurcation and its applications Applied Math Sci volume 19. the computational aspects of the Hopf bifurcation is treated in HASSARD B. WAN Y.H. J Math Anal App 63 297-312 (1978)

[51] NAYFEH and MOOK, Nonlinear Oscillations (1979) WILEY INTERSCIENCE SERIES

[52] NEWELL A.C. and WHITEHEAD J.A. J.Fluid Mech (1969) 38 part 4 667-687

[53] OLVER P.J. Applications of Lie Groups to Differential Equations Springer -Verlag (1986)

[54] ONSAGER L Phys Rev 37 405 (1931) and 38 2265 (1931)

[55] PALM E., WEBER J.E. and KVERNVOLD O. J.Fluid Mech. 54 153 (1972)

[56] ROBERTS J. Math. Anal. App. 1 195-214 (1960)

[57] SCHECTER, R.S. PRIGOGINE I. and HAMM J. R., Phys Fluids 15 379 (1972)

[58] SCHECTER R.S., VERLADE M.G.,and PLATTEN J.K., Adv. Chem. Phys. 26 265 (1974)

[59] SCHECTER R.S. and HIMMELBLAU D.M. phys. fluids 8 8 (1965)

[60] SEGAL L.A. J. Fluid Mech. 38, 203 (1969)

[61] SIMOYI R.H., WOLF A., SWINNEY H. Phys Rev Lett 49 245-8 (1982)

[62] SORET effect. see DE GROOT and MAZUR ref.[14]

[63] STEINBERG V.. Phys. Rev A24 975 1981

[64] STEINBERG V., Phys. Rev A24 2584 1981

[65] STEINBERG V. J. Appl. Math. Mech. (USSR) 35 335 (1971) ANTORANZ J.C., BONILLA L.L., GEA J., VERLADE M.G., Phys Rev Letts 49 1 (1981) ANTORANZ J.C., VERLADE M.G., Phys Rev A 37 4 1381-1382 (1988)

[66] SPARROW C The Lorenz equations bifurcations chaos and strange attractors App. Math Sci vol 41 Springer.

[67] SULLIVAN and AHLERS G., Phys Rev Lett 61, 78 (1988)

[68] TEMAM R. and FOIAS C. J. Math. Pures et Appl. 58 (1979), 339 FOIAS C.J. MANLEY O.P. TEMAM R. and TREVE Y.M. Phys Rev Letts 50 (1983) 1031.

[69] VERONIS J.Fluid Mech. 34 315-336 (1969)

[70] VANDERBAUWHEDE A. DELFT progress report (1988) 12

[71] YAHATA H. Prog. Theo. Phys. Supplement 79, 26 (1984)